

Simple balanced three-manifolds, Heegaard Floer homology and the Andrews-Curtis conjecture

Neda Bagherifard and Eaman Eftekhary

Abstract. The first author introduced a notion of equivalence on a family of 3-manifolds with boundary, called (simple) balanced 3-manifolds in an earlier paper and discussed the analogy between the Andrews-Curtis equivalence for group presentations and the aforementioned notion of equivalence. Motivated by the Andrews-Curtis conjecture, we use tools from Heegaard Floer theory to prove that there are simple balanced 3-manifolds which are not in the trivial equivalence class (i.e. the equivalence class of $S^2 \times [-1, 1]$).

Contents

1	Introduction	2
2	A Heegaard diagram for the mapping torus	6
3	Simplifying computations using algorithmic calculations	9
4	Non-polygonal disks with holomorphic representatives	11
5	The first non-trivial Heegaard-Floer group	16
6	The second non-trivial Heegaard-Floer group	19

1 Introduction

Suppose that $R = \{b_1, \dots, b_m\}$ is a finite subset of the free group $F(X)$ generated by the finite set $X = \{a_1, \dots, a_n\}$. We denote by $(X|R)$ the quotient G of $F(X)$ by the normal subgroup generated by R . The pair (X, R) is then called a *presentation* of G with *generators* X and *relators* R , which is balanced if $|X| = |R|$. An *extended Andrews-Curtis transformation* (EAC-transformation for short) on (X, R) is defined as one of the following transformations, or its inverse, which of course results in another presentation of G [Wri75] (see also [HAM93]):

1. **Composition:** Replace $b \in R$ with bb' for some $b' \neq b$ in R ;
2. **Inversion:** Replace $b \in R$ with b^{-1} ;
3. **Cancellation:** Replace $b = b'aa^{-1}b'' \in R$ with $b'b''$, where $a \in X$ or $a^{-1} \in X$;
4. **Stabilization:** Add a new element a to both X and R ;
5. **Replacement:** Replace $a'a$ or $a'a^{-1}$ for a' in all the relators for some $a \neq a'$ in X .

Stable Andrews-Curtis transformations (or SAC transformations) consist of the first 4 transformations and their inverses. The presentations $P' = (X', R')$ and $P = (X, R)$ are called *EAC equivalent* (respectively, *SAC equivalent*) if P' is obtained from P by a finite sequence of EAC transformations (respectively, SAC transformations). For the trivial group, the SAC equivalence class of a presentation is the same as its EAC equivalence class ([Wri75]). The stable Andrews-Curtis conjecture (or SAC conjecture) states that every balanced presentation of the trivial group is SAC equivalent to the trivial presentation, i.e. (a, a) (c.f. [AC65]). Most experts expect that the SAC conjecture is not true and there are potential counterexamples ([Bro84, BM93, MS99, MMS02]). One of the simplest potential counterexamples for the SAC conjecture is given by $P_0 = (X_0, R_0)$, where

$$X_0 = \{x, y\} \quad \text{and} \quad R_0 = \{r = x^{-1}y^2xy^{-3}, s = y^{-1}x^2yx^{-3}\}, \quad (1)$$

(see [MMS02]). The group presentation P_0 is considered in this paper in correspondence with a notion of equivalence for balanced 3-manifolds, as explained below.

A compact oriented 3-manifold N with boundary is called *balanced* if each component of N has two boundary components of the same genus. Let $\partial^\pm N$ denote boundary components of N where the orientation of $\partial^+ N$ (resp. $\partial^- N$) matches with (resp. is the opposite of) the orientation inherited as the boundary of N . Let $\iota^\pm : \partial^\pm N \rightarrow N$ denote the inclusion maps and H^\pm denotes the normalizer of $\iota_*^\pm(\pi_1(\partial^\pm N))$ in $\pi_1(N)$. A balanced 3-manifold is called *simple* if for each connected component N of it as above, both quotient groups $\pi_1(N)/H^\pm$ are trivial. Associated with each Heegaard diagram $\mathcal{H} = (\Sigma, \boldsymbol{\alpha}, \boldsymbol{\beta})$ of N , there are two balanced presentations $P_\alpha(\mathcal{H})$ and $P_\beta(\mathcal{H})$ for the latter quotient groups where for $P_\alpha(\mathcal{H})$ (resp. $P_\beta(\mathcal{H})$) the generators are in correspondence with the $\boldsymbol{\alpha}$ (resp. $\boldsymbol{\beta}$) and the relators are in correspondence with the $\boldsymbol{\beta}$ (resp. $\boldsymbol{\alpha}$) (see [Bag]). Let $\mathfrak{p}_\alpha(N)$ and $\mathfrak{p}_\beta(N)$ denote the EAC equivalence classes of the presentations $P_\alpha(\mathcal{H})$ and $P_\beta(\mathcal{H})$, respectively. Note that these EAC equivalence classes are independent of the choice of the Heegaard diagram \mathcal{H} for N . Similarly, we may define

$\mathfrak{p}_\alpha(N)$ and $\mathfrak{p}_\beta(N)$ for a balanced 3-manifold N which is not connected. If N is a simple balanced 3-manifold, $\mathfrak{p}_\alpha(N)$ and $\mathfrak{p}_\beta(N)$ are both EAC equivalence classes of presentations for the trivial group.

A notion of equivalence in the family of balanced 3-manifolds was introduced in [Bag]. We say that a balanced 3-manifold N simplifies to another balanced 3-manifold N' if there is an embedded cylinder $C \sim S^1 \times [-1, 1]$ in N , with $\partial^\pm C \sim S^1 \times \{\pm 1\} \subset \partial^\pm N$, such that N' is obtained by cutting N along C and gluing two copies of $D^2 \times [-1, 1]$ to the resulting boundary cylinders in $N \setminus C$. We then write $N \xrightarrow{C} N'$. We say that a balanced 3-manifold N admits a *simplifier* if there is a sequence of simplifications

$$N = N_n \xrightarrow{C_n} N_{n-1} \xrightarrow{C_{n-1}} \cdots \xrightarrow{C_2} N_1 \xrightarrow{C_1} N_0,$$

such that N_0 is a disjoint union of copies of $S^2 \times [-1, 1]$. The inverse of a simplification is called an *anti-simplification*. Two balanced 3-manifolds are called *equivalent* if they may be changed to one-another by a finite sequence of simplifications, anti-simplifications and homeomorphisms. The equivalence of the balanced 3-manifolds N and N' implies that $\mathfrak{p}_\alpha(N) = \mathfrak{p}_\alpha(N')$ and $\mathfrak{p}_\beta(N) = \mathfrak{p}_\beta(N')$. Therefore, a pair of well-defined EAC equivalence classes (of group presentations) are assigned to each equivalence class of balanced 3-manifolds and in this sense, the equivalence notion between balanced 3-manifolds is *weaker* than the EAC equivalence for group presentations. In the family of simple balanced 3-manifolds, both EAC equivalence classes are presentations of the trivial group. Motivated by the SAC conjecture, it is thus natural to ask if there is a simple balanced 3-manifold N which is not equivalent to the trivial simple balanced 3-manifold $S^2 \times [-1, 1]$? In this paper, we combine the main result of [Bag] with tools from Heegaard Floer theory (see [OS04b]) to prove the following theorem.

Theorem 1.1. *There is a simple balanced 3-manifold N with*

$$\mathfrak{p}_\alpha(N) = \mathfrak{p}_\beta(N) = P_0 = [(X_0, R_0)],$$

where P_0 is given in (1), which is not equivalent to $S^2 \times I$.

As mentioned above, besides Heegaard Floer theory, the main tool used in proving Theorem 1.1 is a fundamental result about the equivalence class of the simple balanced 3-manifold $S^2 \times [-1, 1]$, which is proved in [Bag] and may be stated as follows.

Theorem 1.2. [Bag, Theorem 1.6] *Every balanced 3-manifold N which is equivalent to $S^2 \times I$ admits a simplifier.*

The group presentation P_0 of Equation 1 is realized by the Heegaard diagram

$$\overline{\mathcal{H}} = (\overline{\Sigma}, \overline{\boldsymbol{\alpha}} = \{\alpha_1, \alpha_2\}, \overline{\boldsymbol{\beta}} = \{\beta_1, \beta_2\}),$$

illustrated in Figure 1. In fact, the Heegaard diagram $\overline{\mathcal{H}}$ determines a simple balanced 3-manifold N with $\mathfrak{p}_\alpha(N) = \mathfrak{p}_\beta(N) = [P_0]$. If N is equivalent to $S^2 \times I$, Theorem 1.2 implies that

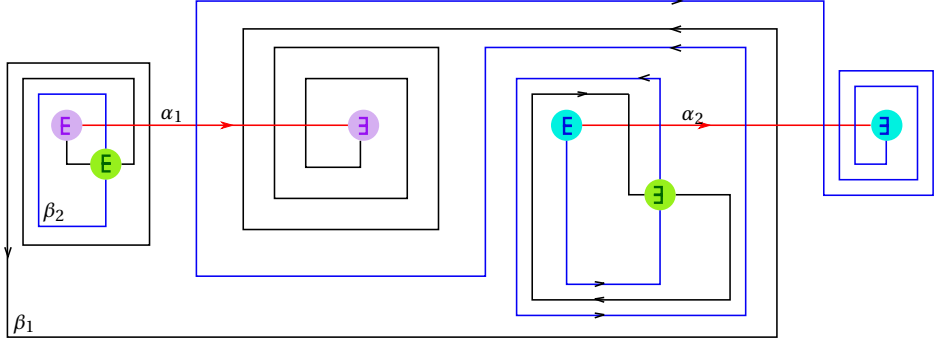


Figure 1. The Heegaard surface is a surface of genus three which is obtained by identifying the boundaries of disks with the same color. The curves are oriented in a way that the balanced presentation associated with this Heegaard diagram is P_0 .

N admits a simplifier. We have $\partial N = \partial^+ N \amalg -\partial^- N$ where $\partial^\pm N$ are surfaces of genus 1. If N admits a simplifier, there is a nontrivial cylinder C in N such that $\partial^\pm C$ in $\partial^\pm N$ are essential curves. Let $f : \partial^+ N \rightarrow \partial^- N$ be the homeomorphism from $\partial^+ N$ to $\partial^- N$ which makes the following diagram commutative:

$$\begin{array}{ccc} H_1(\partial^+ N, \mathbb{Z}) & \xrightarrow{f_*} & H_1(\partial^- N, \mathbb{Z}) \\ & \searrow \iota_*^+ & \swarrow \iota_*^- \\ & H_1(N, \mathbb{Z}) & \end{array}$$

This criteria determines f upto isotopy. Since $\partial^+ C$ is homologous to $\partial^- C$, we may further assume that f maps $\partial^+ C$ to $\partial^- C$. Let N_f denote the closed 3-manifold obtained from N by identifying $\partial^+ N$ with $\partial^- N$ using f . Let \bar{C} denote the torus in M which is obtained from C by identifying $\partial^+ C$ with $\partial^- C$. Thus \bar{C} and $\partial^+ N \sim_f \partial^- N$ represent linearly independent homology classes in $H_2(N_f, \mathbb{Z}) = \mathbb{Z} \oplus \mathbb{Z} \oplus \mathbb{Z}$ with zero Thurston semi-norm. Recall that the Thurston semi-norm of a closed 3-manifold M is defined on $H_2(M, \mathbb{Z})$ by

$$\Theta : H_2(M, \mathbb{Z}) \rightarrow \mathbb{Z}^{\geq 0}, \quad \Theta(\xi) := \min \{ \chi_+(\Sigma) \mid \Sigma \hookrightarrow M \text{ and } [\Sigma] = \xi \},$$

where the minimum is taken over all compact, oriented surfaces $\Sigma = \amalg_i \Sigma_i$ embedded in M and representing the homology class ξ , while $\chi_+(\Sigma)$ is defined by $\sum_{g(\Sigma_i) > 0} (2g(\Sigma_i) - 2)$ (see [Thu86]). Heegaard Floer homology groups with twisted coefficients detect the Thurston semi-norm. More precisely, for a closed 3-manifold M , let $\widehat{HF}(M)$ denote the Heegaard Floer homology group of M with twisted coefficients, which is a $\mathbb{Z}/2\mathbb{Z}$ -graded $\mathbb{Z}_2[H^1(M, \mathbb{Z})]$ -module defined in [OS04b]. There is a decomposition of this group by Spin^c structures,

$$\widehat{HF}(M) = \bigoplus_{\mathfrak{s} \in \text{Spin}^c(M)} \widehat{HF}(M, \mathfrak{s}).$$

Theorem 1.3. [OS04a, Theorem 1.1] For a closed 3-manifold M and $\xi \in H_2(M, \mathbb{Z})$,

$$\Theta(\xi) = \max_{\{\mathfrak{s} \in \text{Spin}^c(M) \mid \widehat{HF}(M, \mathfrak{s}) \neq 0\}} |\langle c_1(\mathfrak{s}), \xi \rangle|.$$

Let us consider the case where $M = N_f$ is given as above. Extend $[\partial^+ N]$ to a basis for $H_2(N_f, \mathbb{Z}) \cong \mathbb{Z}^3$ and consider a corresponding identification of $\text{Spin}^c(M)$ with \mathbb{Z}^3 (by evaluation of the first Chern class of the Spin^c structures over the generators of the homology group $H_2(M, \mathbb{Z}) \cong \mathbb{Z}^3$). In order to prove Theorem 1.1, we show that there are two linearly independent Spin^c structures \mathfrak{s}_1 and \mathfrak{s}_2 , with the property that

$$\langle c_1(\mathfrak{s}_i), [\partial^+ N] \rangle = 0 \quad \text{and} \quad \widehat{HF}(M, \mathfrak{s}_i) \neq 0 \quad \text{for } i = 1, 2.$$

Since $\Theta([\bar{C}]) = 0$, we thus have $[\bar{C}] = \lambda[\partial^+ N]$, for some integer λ , which contradicts our assumption. This shows that N does not have a simplifier and is thus not equivalent to $S^2 \times I$.

A remark about the above argument may be appropriate here. Let us assume that N_1 and N_2 are balanced 3-manifolds and that N_1 simplifies to N_2 , i.e. $N_1 \xrightarrow{C} N_2$. For $k = 1, 2$, let M_k denote the closed 3-manifold obtained by taking two copies N_k^1 and N_k^2 of N_k , identifying $\partial^+ N_k^1$ with $\partial^+ N_k^2$ and identifying $\partial^- N_k^1$ with $\partial^- N_k^2$. Then the cylinder C gives the torus $T \subset M_1$, while M_2 is obtained by cutting M_1 along T and gluing two solid tori to the resulting boundary components. Theorem 1.3 is then helpful in detecting T . Nevertheless, the equivalence of N_1 and N_2 is yet not well-translated to Heegaard Floer theory, e.g. to a practical correspondence between $\widehat{HF}(M_1)$ and $\widehat{HF}(M_2)$. If T is 2-sided, the problem is studied in [Eft15] and [Eft18], and a relatively powerful machinery is developed in [HRW16]. For non-separating T , it is interesting to develop such a correspondence.

About the proof. In Section 2, we construct a Heegaard diagram \mathcal{H} for the closed manifold M from \mathcal{H} , following the approach of [Lek13]. The number of generators for the Heegaard diagram \mathcal{H} is 7936, and it is thus not feasible to find the Spin^c structures \mathfrak{s}_1 and \mathfrak{s}_2 and compute the groups $\widehat{HF}(M, \mathfrak{s}_i)$ without computational assistance (from computers). We prove a simple lemma from linear algebra in Section 3, in the spirit of the general discussion in [Eft15, Section 2]. The lemma is used, in combination with a computer program, to obtain a short-list of potential Spin^c structures \mathfrak{s} with $\widehat{HF}(M, \mathfrak{s}) \neq 0$ (although obtaining the short-list is not an official part of our argument). Among the potential candidates, two specific Spin^c structures \mathfrak{s}_1 and \mathfrak{s}_2 are considered in Section 5 and Section 6. The chain complexes associated with these Spin^c structures are 8-dimensional and 72-dimensional, respectively. The homology groups of the chain complexes $\widehat{CF}(M, \mathfrak{s}_i)$ (for $i = 1, 2$) are studied using the lemma proved in Section 3, a series of computer assisted computations and explicit computations of the contribution of moduli spaces associated with certain classes of Whitney disks. Since the Heegaard diagram is not nice (in the sense of [SW10]), such explicit computations are necessary and appear in Section 4.

2 A Heegaard diagram for the mapping torus

In this section, we obtain a Heegaard diagram for $M = N_f$, using the construction of [Lek13]. Let us assume that the diagram $\overline{\mathcal{H}}$ is obtained from a Morse function $h : N \rightarrow [-1, 1]$. Then h gives a circle-valued Morse function $\bar{h} : M \rightarrow S^1$ with two critical points x_1 and x_2 of index 1 and two critical points y_1 and y_2 of index 2, such that

$$\begin{aligned} N_{x_1}^u(h) \cap \Sigma = \alpha_1, & \quad N_{x_2}^u(h) \cap \Sigma = \alpha_2, & \quad N_{y_1}^s(h) \cap \Sigma = \beta_1, & \quad N_{y_2}^s(h) \cap \Sigma = \beta_2, \\ \bar{h}^{-1}(1) = \partial^+ N \sim_f \partial^- N = \Sigma_{min} & \quad \text{and} & \quad \bar{h}^{-1}(-1) = \bar{\Sigma} = \Sigma_{max}. \end{aligned}$$

Here N_x^s and N_x^u denote the stable and unstable manifold of $x \in N$ with respect to the flow of a gradient-like vector field for h . Following [Lek13], let p_1 and p_2 be disjoint points in $\bar{\Sigma} \setminus \alpha \cup \beta$ and γ_1 and γ_2 denote two gradient flow lines disjoint from $N_{x_i}^u$ and $N_{y_i}^s$ such that

$$\gamma_i \cap \bar{\Sigma} = \{p_i\} \quad \text{and} \quad \gamma_i \cap \partial^+ N = \{\bar{p}_i\}, \quad \text{for } i = 1, 2.$$

Furthermore, γ_1 (resp. γ_2) is mapped onto the northern (resp. southern) semi-circle of S^1 . Let $N(\gamma_i)$, $i = 1, 2$, denote the normal neighborhood of γ_i that intersects $\bar{\Sigma}$ and $\partial^+ N$ in the small disks D_{p_i} and $D_{\bar{p}_i}$, respectively. By removing $D_{p_i}^\circ$ and $D_{\bar{p}_i}^\circ$ and gluing ∂D_{p_i} to $\partial D_{\bar{p}_i}$ along $\partial N(\gamma_i)$ we obtain the Heegaard surface Σ . Let $\alpha_5 = \partial D_{\bar{p}_1}$ and $\beta_5 = \partial D_{p_2}$. Let α'_3 and α'_4 (resp. β'_3 and β'_4), be disjoint arcs in $\partial^+ N$ such that $\partial\alpha'_3$ and $\partial\alpha'_4$ are disjoint points on β_5 and $\partial\beta'_3$ and $\partial\beta'_4$ are disjoint points on α_5 , while $|\alpha'_3 \cap \beta'_4| = |\alpha'_4 \cap \beta'_3| = 1$ and $|\alpha'_3 \cap \beta'_3| = |\alpha'_4 \cap \beta'_4| = 0$. Flowing the arcs β'_3 and β'_4 through the gradient flow of \bar{h} above the northern semi-circle, we obtain disjoint arcs β''_3 and β''_4 in $\Sigma \setminus \partial^+ N$ which are disjoint from β_1 and β_2 . Similarly, flowing the arcs α'_3 and α'_4 , we obtain α''_3 and α''_4 which are disjoint from α_1 and α_2 . This determines the sets of α and β curves:

$$\alpha = \{\alpha_1, \alpha_2, \alpha_3 = \alpha'_3 \cup \alpha''_3, \alpha_4 = \alpha'_4 \cup \alpha''_4, \alpha_5\} \quad \text{and} \quad \beta = \{\beta_1, \beta_2, \beta_3 = \beta'_3 \cup \beta''_3, \beta_4 = \beta'_4 \cup \beta''_4, \beta_5\}.$$

Having fixed a marked point z , finger-move isotopies may be used to make $(\Sigma, \alpha, \beta, z)$ weakly admissible. If we apply the procedure to the Heegaard diagram of Figure 1, we arrive at the admissible Heegaard diagram illustrated in Figure 2 with 21392 generators. Handle-slides of α_4 over α_3 (10 times) and isotopies on α_3 give an alternative (more suitable) weakly admissible Heegaard diagram \mathcal{H} with 7936 generators, as illustrated in Figure 3. We use $x_{i,j,k}$ to label the intersection point of α_i and β_j which is labeled k in the diagram of Figure 3.

The set of periodic domains for \mathcal{H} is generated by three domains P_1 , P_2 and P_3 . The first two generators are shown in Figure 3. The periodic domains P_1 and P_2 are of the form

$$P_1 = -D_{52} + \sum_{i=53}^{57} D_i + \sum_{i \in I_1} D_i \quad \text{and} \quad P_2 = -D_{49} + \sum_{i \in I_2} D_i + \sum_{i \in I_1} D_i,$$

where the domains D_i with i in I_1 and I_2 are colored gray and green in Figure 3, respectively. If $\partial_b P$ denote the β -boundary of a periodic domain P , we then have $\partial_b(P_1) = -\beta_5$ and

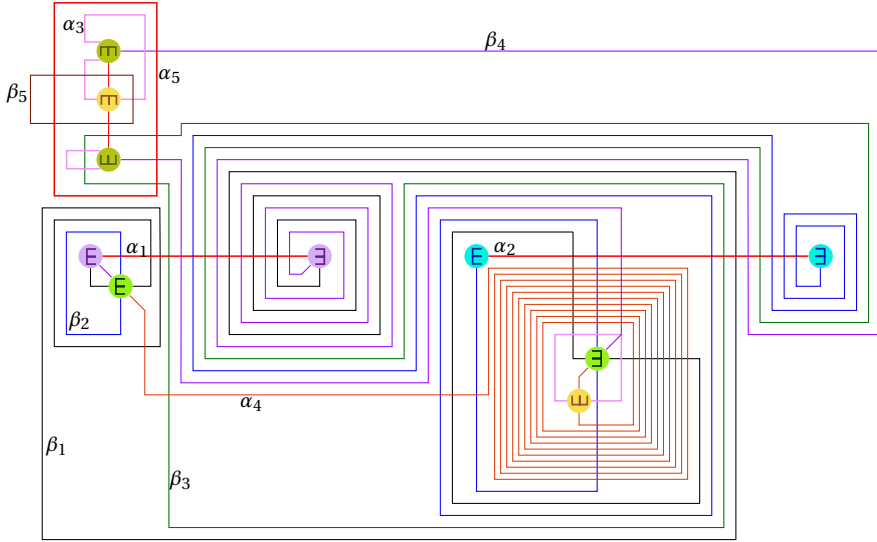


Figure 2. A weakly admissible Heegaard diagram of N_f with 21392 generators

$\partial_b(P_2) = \beta_3$. We may choose the third generator P_3 of the space of periodic domains so that $\partial_b(P_3) = \beta_4 + 2\beta_3 - 3\beta_1 + 2\beta_2$. Let $H(P_i) \in H_2(M, \mathbb{Z})$ denote the homology classes associated with the periodic domains P_i for $i = 1, 2, 3$, which form a basis for $H_2(M, \mathbb{Z})$ (see [OS04b], Proposition 2.15). Correspondingly, we obtain a bijection

$$c : \text{Spin}^c(M) \rightarrow \mathbb{Z} \oplus \mathbb{Z} \oplus \mathbb{Z}, \quad c(\mathfrak{s}) := \frac{1}{2}(\langle c_1(\mathfrak{s}), H(P_1) \rangle, \langle c_1(\mathfrak{s}), H(P_2) \rangle, \langle c_1(\mathfrak{s}), H(P_3) \rangle),$$

which gives an identification of $\text{Spin}^c(M)$ with \mathbb{Z}^3 . To compute $\mathfrak{s}_z : \mathbb{T}_\alpha \cap \mathbb{T}_\beta \rightarrow \text{Spin}^c(M) = \mathbb{Z}^3$ under this identification, define $\mathfrak{s}_z^r : \mathbb{T}_\alpha \cap \mathbb{T}_\beta \rightarrow \mathbb{Z}^3$ by setting $\mathfrak{s}_z^r(x_0) = (0, 0, 0)$ for

$$x_0 = (x_i^0)_{i=1}^5 = (x_{1,1,1}, x_{2,2,1}, x_{3,4,1}, x_{4,5,1}, x_{5,3,2}).$$

Let $(y_i^0)_{i=1}^5$ denote a permutation of $(x_i^0)_{i=1}^5$ so that $y_i^0 \in \beta_i$. Fix a connected path γ_0 on $\alpha \cup \beta$ in the diagram such that for each $\alpha \in \boldsymbol{\alpha}$ and $\beta \in \boldsymbol{\beta}$, $\gamma_0 \cap \alpha$ and $\gamma_0 \cap \beta$ are connected and $x_i^0 \in \gamma_0$, $1 \leq i \leq 5$, (the yellow path in Figure 3 satisfies these properties). Fix

$$x = (x_i)_{i=1}^5 = (y_i)_{i=1}^5 \in \mathbb{T}_\alpha \cap \mathbb{T}_\beta \quad \text{with } x_i \in \alpha_i \text{ and } y_i \in \beta_i,$$

i.e. $(y_i)_i$ is just a permutation of $(x_i)_i$. Let $\epsilon(x_0, x)$ denote the closed 1-cycle in Σ obtained by connecting y_i to y_i^0 through β_i , connecting y_i^0 to x_i^0 through γ_0 , and connecting x_i^0 to x_i through α_i for $i = 1, \dots, 5$. Note that for $j = 1, 2, 3$, the evaluation $\langle PD[\epsilon(x_0, x)], H(P_j) \rangle$ is the algebraic intersection number of $\epsilon(x_0, x)$ with $\partial_b P_j$. Therefore, if we set

$$\mathfrak{s}_z^r(x) := (-\langle \epsilon(x_0, x), \beta_5 \rangle, \langle \epsilon(x_0, x), \beta_3 \rangle, \langle \epsilon(x_0, x), \beta_4 + 2\beta_3 - 3\beta_1 + 2\beta_2 \rangle),$$

there is a fixed triple $(a, b, c) = (0, -1, -4) \in \mathbb{Z}^3$ such that $\mathfrak{s}_z = \mathfrak{s}_z^r(x) + (a, b, c)$. In the definition of \mathfrak{s}_z^r , note that the intersection numbers take place over the Heegaard surface. The map \mathfrak{s}_z^r is used instead of \mathfrak{s}_z for the purposes of this paper.

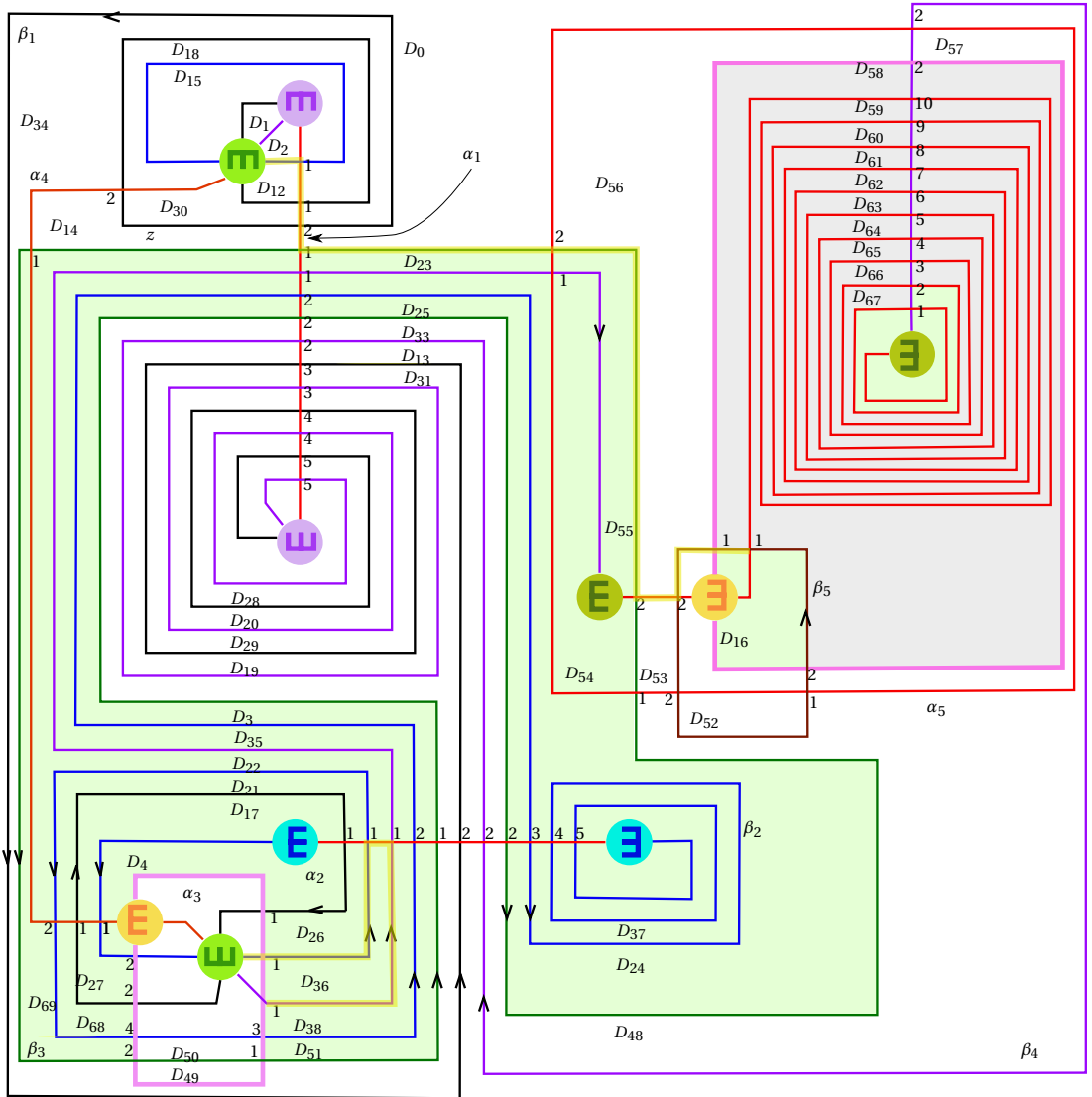


Figure 3. A weakly admissible Heegaard diagram for M with 7936 generators. The connected components of $\Sigma \setminus \alpha \cup \beta$ are labeled D_i , for $i = 0, \dots, 67$. The periodic domains are generated by $P_1 = -D_{52} + \sum_{i=53}^{57} D_i + \sum_{i \in I_1} D_i$, $P_2 = -D_{49} + \sum_{i \in I_2} D_i + \sum_{i \in I_1} D_i$ and a third periodic domain P_3 , where D_i is colored gray for $i \in I_1$ and green for $i \in I_2$. We have $\partial_b(P_1) = -\beta_5$ and $\partial_b(P_2) = \beta_3$. The periodic domain P_3 may be chosen so that $\partial_b(P_3) = \beta_4 + 2\beta_3 - 3\beta_1 + 2\beta_2$.

3 Simplifying computations using algorithmic calculations

All our computations are performed with coefficients in $\mathbb{Z}_2[H^1(M, \mathbb{Z})]$. In the discussions of this section, we have the diagram $\mathcal{H} = (\Sigma, \boldsymbol{\alpha}, \boldsymbol{\beta}, z)$ from Figure 3 in mind. Nevertheless, the strategy works for many of the chain complexes associated with sutured manifold diagrams in the sense of [Juh06], or even [AE15]. Since there is a large number of generators associated with \mathcal{H} , we break the computation of $\widehat{HF}(M)$ into a computer-assisted part and a human part using the following observation.

Let $\mathbf{z}_2 \subset \mathbf{z}_1$ denote two sets of marked points containing z . Most of the time, we take $\mathbf{z}_2 = \{z\}$. If \mathbf{z}_1 is sufficiently large so that it contains a marked point in each one of the periodic domains, we may choose a decomposition $\widehat{CF}(\Sigma, \boldsymbol{\alpha}, \boldsymbol{\beta}, \mathbf{z}_1) = A \oplus B \oplus H$, so that the differentials $d_{\mathbf{z}_1}$ and $d_{\mathbf{z}_2} = d_{\mathbf{z}_1} + d'$ are determined by the matrices

$$d_{\mathbf{z}_1} = \begin{pmatrix} 0 & 0 & 0 \\ I & 0 & 0 \\ 0 & 0 & 0 \end{pmatrix} \quad \text{and} \quad d' = \begin{pmatrix} f & h & m \\ k & g & n \\ p & q & l \end{pmatrix}. \quad (2)$$

Lemma 3.1. *Suppose that with the above notation in place, $I + k$ is invertible. Then*

$$H_*(\widehat{CF}(\Sigma, \boldsymbol{\alpha}, \boldsymbol{\beta}, \mathbf{z}_2)) = H_*(H, l + p(I + k)^{-1}n).$$

Proof. The proof follows from two base changes. The first base change is given by

$$\begin{aligned} & \begin{pmatrix} I + k & (I + k)f(I + k)^{-1} & 0 \\ 0 & I & 0 \\ 0 & 0 & I \end{pmatrix} \begin{pmatrix} f & h & m \\ I + k & g & n \\ p & q & l \end{pmatrix} \begin{pmatrix} (I + k)^{-1} & f(I + k)^{-1} & 0 \\ 0 & I & 0 \\ 0 & 0 & I \end{pmatrix} \\ &= \begin{pmatrix} 0 & * & m' \\ I & * & n \\ p(I + k)^{-1} & * & l \end{pmatrix} = \begin{pmatrix} 0 & m'A & m' \\ I & nA & n \\ A & lA & l \end{pmatrix}, \end{aligned}$$

where $A = p(I + k)^{-1}$ and the last equality follows from $d_{\mathbf{z}_2}^2 = 0$. The second base change is

$$\begin{pmatrix} I & 0 & 0 \\ 0 & I & 0 \\ 0 & A & I \end{pmatrix} \begin{pmatrix} 0 & m'A & m' \\ I & nA & n \\ A & lA & l \end{pmatrix} \begin{pmatrix} I & 0 & 0 \\ 0 & I & 0 \\ 0 & A & I \end{pmatrix} = \begin{pmatrix} 0 & 0 & m' \\ I & 0 & n \\ 0 & 0 & l + An \end{pmatrix}.$$

□

In applications of Lemma 3.1, we choose an area assignment \mathcal{A} for the regions in $\Sigma \setminus \boldsymbol{\alpha} \cup \boldsymbol{\beta}$ such that $\mathcal{A}(P_i) = 0$ for $i = 1, 2, 3$. Moreover, $\mathbf{z}_1, \mathbf{z}_2$ and \mathcal{A} are chosen so that the regions not touched by \mathbf{z}_1 have very small areas and the regions containing marked points from $\mathbf{z}_1 \setminus \mathbf{z}_2$

have very large areas. Under these assumptions, in each Spin^c class \mathfrak{s} , \mathcal{A} descends to an energy filtration on $\widehat{CF}(\Sigma, \boldsymbol{\alpha}, \boldsymbol{\beta}, \mathbf{z}_2, \mathfrak{s})$ (see [OS04b]). We may further assume that

$$A = \langle a_1, \dots, a_r \rangle, \quad B = \langle b_1, \dots, b_r \rangle, \quad \text{with } \mathcal{A}(a_1) < \mathcal{A}(a_2) < \dots < \mathcal{A}(a_r),$$

while the differential $d_{\mathbf{z}_1}$ is given by sending a_i to b_i . With respect to the energy filtration, $\mathcal{A}(a_i) - \mathcal{A}(b_i)$ is then a small positive number and k is a lower triangular matrix with zeros on the diagonal. Therefore, $I+k$ is an invertible matrix with $(I+k)^{-1} = \sum_{i=0}^{\infty} k^i$. This allows us use Lemma 3.1. Of course, the use of Lemma 3.1 is not restricted to the aforementioned situation.

In our search for the Spin^c classes \mathfrak{s} with the property that $\widehat{HF}(M, \mathfrak{s}) \neq 0$, we may first restrict our attention to the Spin^c classes which satisfy $\langle c_1(\mathfrak{s}), H(P_1) \rangle = 0$, since P_1 corresponds to $\partial^+ N$ and is represented by an embedded surface of genus 1. We may then enlarge the set $\mathbf{z}_2 = \{z\}$ of punctures in the Heegaard diagram to a bigger set \mathbf{z}_1 , so that $(\Sigma, \boldsymbol{\alpha}, \boldsymbol{\beta}, \mathbf{z}_1)$ is nice, while the criteria discussed in the previous two paragraphs is satisfied. If the group

$$H_*(\widehat{HF}(\Sigma, \boldsymbol{\alpha}, \boldsymbol{\beta}, \mathbf{z}_1, \mathfrak{s}))$$

is trivial, it follows that $\widehat{HF}(M, \mathfrak{s})$ is also trivial. Trying different sets \mathbf{z}_1 of marked points allows us exclude many of the Spin^c classes \mathfrak{s} from the the Thurston polytope, consisting of Spin^c structures \mathfrak{t} with $\widehat{HF}(M, \mathfrak{t}) \neq 0$. Among the remaining Spin^c classes, we combine Lemma 3.1, computer assisted computations and the study of certain classes of Whitney disks (from next section) to show that $\widehat{HF}(M, \mathfrak{s}_i) \neq 0$ for $i = 1, 2$, where \mathfrak{s}_1 and \mathfrak{s}_2 are the classes of generators x_1 and x_2 of $\widehat{CF}(\mathcal{H})$ with

$$\mathfrak{s}_z^r(x_1) = (0, 1, 7) \quad \text{and} \quad \mathfrak{s}_z^r(x_2) = (0, -1, -8),$$

respectively. As we will see in Section 5 and Section 6, there are 8 generators x_1 and 72 generators x_2 of the above type.

4 Non-polygonal disks with holomorphic representatives

In this section, we study the moduli spaces associated with three classes of Whitney disks with non-polygonal domains, which will be encountered in Section 6. First, let $D_{k,l,n} = D(\phi_{k,l,n})$ denote the genus zero domain of a Whitney disk $\phi_{k,l,n}$, with two boundary components having $2k$ -edges and $2l$ -edges, respectively. The edges on each boundary component consist of alternating arcs from distinct α and β curves. For such a disk to have Maslov index 1, it is necessary that all the $2(k+l)$ angles on the boundary are acute angles, except for precisely one of them. We further assume that the obtuse angle is on the boundary component with $2l$ edges, where α_1 and β_1 meet at x_n and enter the interior of $D_{k,l,n}$, and intersect each other at x_{n-1}, \dots, x_1 in $D_{k,l,n}^\circ$. There is some extra freedom in choosing the domain $D_{k,l,n}$ (up to isotopy of the curves) which corresponds to the edges where α_1 and β_1 exit $D_{k,l,n}$ and is dropped from the notation (see Figure 4 (left)).

Lemma 4.1. *Let $\phi_{k,l,n}$ be a disk with a domain as described above. Then $\#\widehat{M}(\phi_{k,l,n}) = 1$.*

Proof. First, consider the case $k = l = 1$. Consider the triply punctured Heegaard diagram

$$\mathcal{H}_1 = \mathcal{H}_1^n = (\Sigma_1, \boldsymbol{\alpha}_1 = \{\alpha_1, \alpha_2, \alpha_3\}, \boldsymbol{\beta}_1 = \{\beta_1, \beta_2, \beta_3\}, z_1, z_2, z_3)$$

illustrated in Figure 4 (right). Here Σ_1 is a surface of genus three and the sutured manifold determined by \mathcal{H}_1 is the same as the sutured manifold determined by a Heegaard diagram $(T = S^1 \times S^1, \alpha, \beta = \{b\} \times S^1, z_1, z_2)$, where α is homotopically trivial and cuts β twice, one of the punctures is located in one of the two bigons in $T - \alpha - \beta$, and two of the punctures

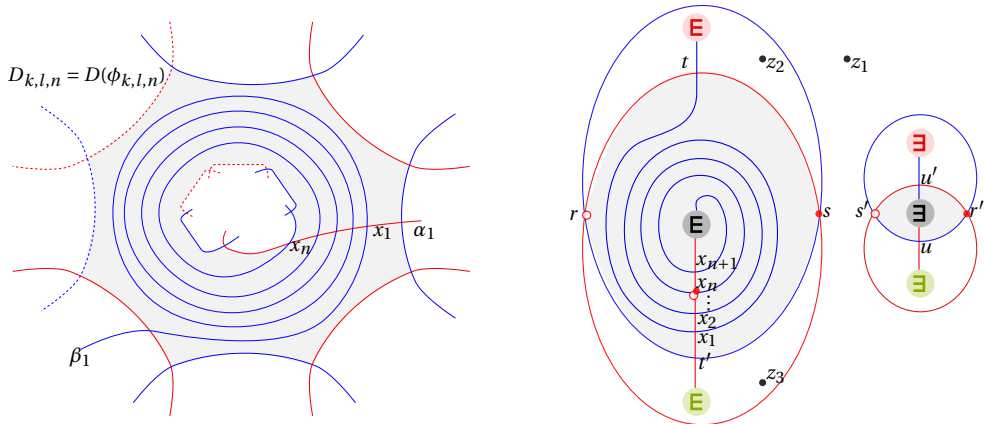


Figure 4. Part of a Heegaard diagram which illustrates the domain associated with the disk $\phi_{k,l,n}$ is illustrated (left). The red curves are the α curves and the blue curves are the β curves. A Heegaard diagram of genus 3 containing the domain $D_{1,1,n}$ is illustrated on the right. The domain of the Whitney disk $\psi \in \pi_2(R_n, U_n)$ is shaded.

are located in the cylindrical component of $T - \alpha - \beta$. Therefore, the Heegaard Floer group associated with \mathcal{H}_1 is trivial. With the notation of Figure 4, the generators in $\mathbb{T}_\alpha \cap \mathbb{T}_\beta$ are

$$\begin{aligned} R_i &= (x_i, r, r'), & S_i &= (x_i, r, s'), & T_i &= (x_i, s, r'), & U_i &= (x_i, s, s'), & i &= 1, \dots, n+1 \\ V &= (t, t', r'), & W &= (t, t', s'), & X &= (u, r, u'), & Y &= (u, s, u'). \end{aligned}$$

Most Whitney disks with positive domain and index 1 which contribute to the differential are of the form $\phi_{1,1,k}$ for some $k = 1, \dots, n$. In fact, there are Whitney disks

$$\psi_k^1 \in \pi_2(U_k, S_{k+1}), \quad \psi_k^2 \in \pi_2(T_k, R_{k+1}), \quad \psi_{n+1-k}^3 \in \pi_2(R_{k+1}, S_k) \quad \text{and} \quad \psi_{n+1-k}^4 \in \pi_2(T_{k+1}, U_k)$$

for $k = 1, \dots, n$, where each ψ_k^i is of type $\phi_{1,1,k}$. Other than these classes, there are also disks

$$\psi_0^1 \in \pi_2(V, R_1), \quad \psi_0^2 \in \pi_2(W, S_1), \quad \psi_0^3 \in \pi_2(X, S_{n+1}) \quad \text{and} \quad \psi_0^4 \in \pi_2(Y, U_{n+1}),$$

with Maslov index one, and the domain of every one of them is a rectangle. Therefore, $\#\widehat{M}(\psi_0^i) = 1$ for $i = 1, \dots, 4$. Moreover, there are disks $\phi \in \pi_2(T_1, W)$ and $\phi' \in \pi_2(T_{n+1}, X)$ with domains of type $\phi_{1,2,n}$. If we set

$$m = \#\widehat{M}(\phi), \quad m' = \#\widehat{M}(\phi') \quad \text{and} \quad m_k^i = \#\widehat{M}(\psi_k^i) \quad \text{for } i = 1, \dots, 4 \text{ and } k = 0, \dots, n,$$

it follows that $m_0^i = m_1^i = 1$ and that the differential of the chain complex is given by

$$\begin{array}{ccccccc} T_k & \xrightarrow{m_k^2} & R_{k+1} & & T_1 & \xrightarrow{1} & R_2 & & T_{n+1} & \xrightarrow{m'} & X & & Y & & V \\ m_{n+2-k}^4 \downarrow & & \downarrow m_{n+1-k}^3 & & m \downarrow & & \downarrow m_n^3 & & 1 \downarrow & & \downarrow 1 & & 1 \downarrow & & 1 \downarrow \\ U_{k-1} & \xrightarrow{m_{k-1}^1} & S_k & & W & \xrightarrow{1} & S_1 & & U_n & \xrightarrow{m_n^1} & S_{n+1} & & U_{n+1} & & R_1 \end{array}$$

for $k = 2, \dots, n$. Therefore, we conclude that $m = m_n^3$, $m' = m_n^1$ and

$$m_k^2 \cdot m_{n+1-k}^3 = m_{n+2-k}^4 \cdot m_{k-1}^1 \quad \text{for } k = 2, \dots, n. \quad (3)$$

For $n = 2$, (3) implies $m_2^2 = m_2^4$. Moreover, since the homology is trivial, $m_2^2 = m_2^4 = 1$. This proves the claim for $\phi_{1,1,2}$. Having established the proof for $\phi_{1,1,j}$ with $j = 1, \dots, n-1$ (where $n > 2$), Equation (3) for $k = 2$ implies that $m_n^4 = 1$, proving the claim for $\phi_{1,1,n}$.

Next, we consider the case $l = 1$ while k is arbitrary. Let

$$\mathcal{H}_2 = (\Sigma_2, \boldsymbol{\alpha}_2 = \{\alpha_0, \alpha_1, \dots, \alpha_{k+1}\}, \boldsymbol{\beta}_2 = \{\beta_0, \beta_1, \dots, \beta_{k+1}\}, z)$$

be the Heegaard diagram shown in Figure 5. Here Σ_2 is a surface of genus $k+3$. With the notation of Figure 5 in place and refreshing the notation set for the case $k = l = 1$, the generators in $\mathbb{T}_\alpha \cap \mathbb{T}_\beta$ are

$$\begin{aligned} W &= (v, r, u_2, \dots, u_k, r'), & V &= (s, t_k, u_2, \dots, u_{t-1}, s', t_t, \dots, t_{k-1}, r'), & R_i &= (u'_1, r, u_2, \dots, u_k, x_i), \\ S_i &= (t'_1, r, u_2, \dots, u_k, x_i), & T_i &= (s, t_k, t_1, \dots, t_{k-1}, x_i) \quad \text{and} & U_i &= (s, u_1, u_2, \dots, u_k, x_i), \end{aligned}$$

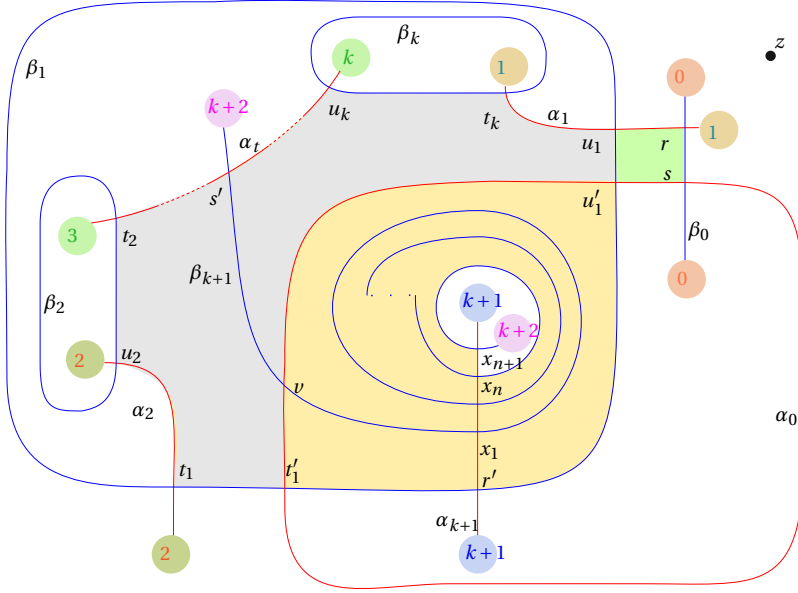


Figure 5. A Heegaard surface of genus $k+3$. The colored region denotes the domain associated with ψ , which degenerates in two ways as $\phi_{1,1,n} * \phi$ and $\phi' * \phi_{k,1,n}$, where $D(\phi')$ is the region colored green and $D(\phi_{1,1,n})$ is the union of regions colored yellow.

where i belongs to $\{1, \dots, n+1\}$. Consider the Whitney disks

$$\phi_{1,1,n} \in \pi_2(R_n, S_{n+1}), \quad \phi \in \pi_2(S_{n+1}, T_{n+1}), \quad \phi' \in \pi_2(R_n, U_n), \quad \phi_{k,1,n} \in \pi_2(U_n, T_{n+1}).$$

such that $D(\phi')$ is the green domain, $D(\phi_{1,1,n})$ is the union of yellow domains, $D(\phi)$ is the union of grey and green domains and $D(\phi_{k,1,n})$ is the union of grey and yellow domains. Then $\psi = \phi_{1,1,n} * \phi = \phi' * \phi_{k,1,n}$ has index 2, while these are the only degenerations of ψ as a juxtaposition of two positive Whitney disks of Maslov index 1. This implies

$$\#\widehat{M}(\phi_{k,1,n}) = \#\widehat{M}(\phi_{k,1,n}) \cdot \#\widehat{M}(\phi') = \#\widehat{M}(\phi_{1,1,n}) \cdot \#\widehat{M}(\phi) = \#\widehat{M}(\phi_{1,1,n}) = 1,$$

completing the proof for the case where $l = 1$, while k and n are arbitrary. Similarly, the argument above may be used to conclude $\#\widehat{M}(\phi_{k,l,n}) = 1$ for arbitrary values of k, l and n . \square

Let $D(\phi_{n,m})$ denote the genus zero domain of a Whitney disk $\phi_{n,m}$ which has three boundary components, each consisting of 2 edges on α_i and β_i for $i = 1, 2, 3$. Let α_3 have n intersection points $\{x_1, \dots, x_n\}$ with β_3 and α_2 have m intersection points $\{y_1, \dots, y_m\}$ with β_2 in $D(\phi_{n,m})$. The union of the yellow regions and the grey regions in Figure 6 illustrates the domain of such a disk. We assume that all the corners of the boundary edges in $D(\phi_{n,m})$ are acute except for two, where α_2 intersects β_2 in an obtuse angle in y_{m-1} and α_3 intersects β_3 in an obtuse angle in x_{n-1} (see Figure 6).

Lemma 4.2. *If the domain of $\phi_{n,m}$ is as described above, we have $\#\widehat{M}(\phi_{n,m}) = 1$.*

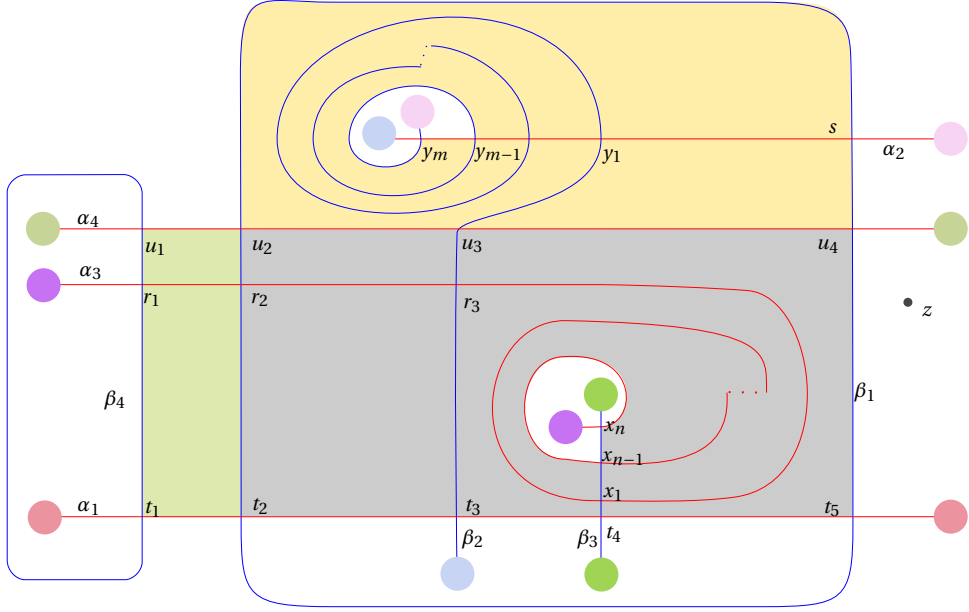


Figure 6. A Heegaard surface of genus 6. The colored regions denote the domain associated with a Whitney disk ψ of index 2 which degenerates in two ways.

Proof. Consider the Heegaard diagram

$$\mathcal{H}_3 = (\Sigma, \boldsymbol{\alpha} = \{\alpha_1, \alpha_2, \alpha_3, \alpha_4\}, \boldsymbol{\beta} = \{\beta_1, \beta_2, \beta_3, \beta_4\}, z)$$

which is illustrated in Figure 6. Here Σ is a surface of genus six which is obtained by attaching six one-handles that each one connects the boundary circles of disks with the same color. There are $4nm + 3m + 2n + 2$ intersection points in $\mathbb{T}_{\boldsymbol{\alpha}} \cap \mathbb{T}_{\boldsymbol{\beta}}$. With the notation of Figure 6 in place, these intersection points are

$$\begin{aligned} P &= (t_4, u_1, r_3, s), & Q &= (t_4, u_3, r_1, s) & R_i &= (t_1, u_3, x_i, s), & S_i &= (t_3, u_1, x_i, s), \\ T_{i,j} &= (t_2, u_1, x_i, y_j), & U_{i,j} &= (t_5, u_1, x_i, y_j), & V_{i,j} &= (t_1, u_2, x_i, y_j), & W_{i,j} &= (t_1, u_4, x_i, y_j) \\ X_j &= (t_4, u_2, r_1, y_j), & Y_j &= (t_4, u_4, r_1, y_j) & \text{and} & & Z_j &= (t_4, u_1, r_2, y_j), \end{aligned}$$

for $i = 1, \dots, n$ and $j = 1, \dots, m$. Consider the Whitney disks of index 1

$$\begin{aligned} \phi_{1,1,m-1} &\in \pi_2(V_{n-1,m-1}, W_{n-1,m}), & \phi_{2,1,n-1} &\in \pi_2(W_{n-1,m}, U_{n,m}), \\ \phi &\in \pi_2(V_{n-1,m-1}, T_{n-1,m-1}) & \text{and} & & \phi_{n,m} &\in \pi_2(T_{n-1,m-1}, U_{n,m}) \end{aligned}$$

Here, the domains $D(\phi_{1,1,m-1})$ is the union of the regions colored yellow, $D(\phi)$ is the union of the regions colored green, $D(\phi_{2,1,n-1})$ is the union of the regions colored grey and green, and $D(\phi_{n,m})$ is the union of the regions colored yellow and grey in Figure 6. Then

$$\psi = \phi_{1,1,m-1} * \phi_{2,1,n-1} = \phi * \phi_{n,m},$$

determined by $D(\psi)$ which is the union of all colored regions, is a Whitney disk of Maslov index 2 in $\pi_2(V_{n-1,m-1}, U_{n,m})$. The disk ψ degenerates as the juxtaposition of two disks of Maslov index 1 only in the above two ways. Therefore, we conclude that

$$\#\widehat{M}(\phi_{n,m}) = \#\widehat{M}(\phi_{n,m}) \cdot \#\widehat{M}(\phi) = \#\widehat{M}(\phi_{1,1,m-1}) \cdot \#\widehat{M}(\phi_{2,1,n-1}) = 1.$$

The last equality, which follows from Lemma 4.1, completes the proof of the lemma. \square

For $\phi \in \pi_2(x, y)$, let $D(\phi)$ be a surface of genus one with one boundary component consisting of 2 edges that contains a unique intersection point u in the interior which belongs to both x and y (see Figure 7). The grey domains on the left illustrate $D(\phi)$.

Lemma 4.3. *Let ϕ be a disk with a domain as described above. Then $\#\widehat{M}(\phi) = 1$.*

Proof. Consider the triply punctured Heegaard diagram

$$\mathcal{H}_4 = (\Sigma, \boldsymbol{\alpha} = \{\alpha_1, \alpha_2\}, \boldsymbol{\beta} = \{\beta_1, \beta_2\}, \mathbf{z} = \{z_1, z_2, z_3\})$$

of genus 1 which is illustrated in Figure 7 (left). With the notation of Figure 7 in place, there are 6 intersection points in $\mathbb{T}_{\boldsymbol{\alpha}} \cap \mathbb{T}_{\boldsymbol{\beta}}$, which may be listed as

$$R_1 = (x, u), \quad R_2 = (y, u), \quad S_1 = (t, v), \quad S_2 = (t, w), \quad T_1 = (s, v) \quad \text{and} \quad T_2 = (s, w).$$

The differential is shown in Figure 7, on the right. A black arrow which connects a generator X to a generator Y denotes that there is a disk from X to Y with a unique holomorphic representative. The arrow in purple denotes the disk with the domain $D(\phi)$. By doing an isotopy which removes the two intersection points of β_2 with α_1 and then doing a destabilization which removes α_2 and β_2 , we obtain the standard genus zero Heegaard diagram for the closed three manifold $S^1 \times S^2$. Therefore the Heegaard Floer homology group associated with \mathcal{H} is \mathbb{Z}^2 . This proves that $\#\widehat{M}(\phi) = 1$. \square

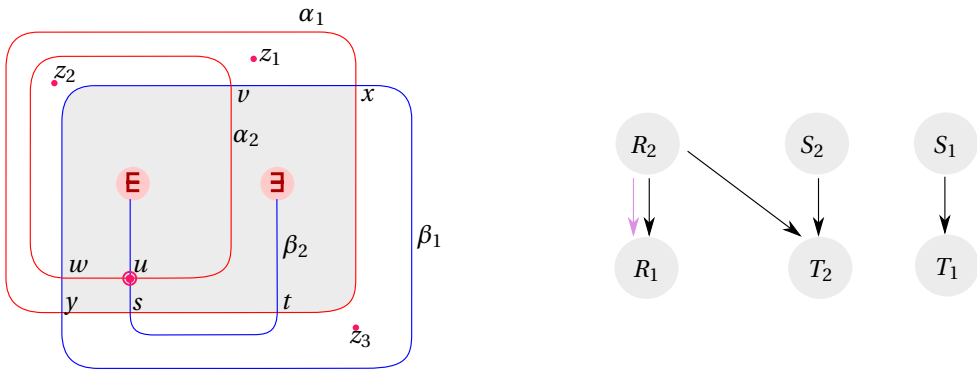


Figure 7. Left: A Heegaard diagram with three marked points and a Heegaard surface of genus one. Right: the differential associated with this diagram.

5 The first non-trivial Heegaard-Floer group

Let us assume that \mathfrak{s}_1 corresponds to the triple $(0, 1, 7)$. The chain complex $\widehat{CF}(M, \mathfrak{s}_1)$ is then generated by the following 8 generators:

$$\begin{aligned} \textcircled{1} &= \{x_{1,1,2}, x_{2,2,5}, x_{3,3,1}, x_{4,5,2}, x_{5,4,2}\} & \textcircled{2} &= \{x_{1,1,2}, x_{2,2,5}, x_{3,3,2}, x_{4,5,2}, x_{5,4,2}\} \\ \textcircled{3} &= \{x_{1,1,2}, x_{2,4,2}, x_{3,2,1}, x_{4,5,2}, x_{5,3,2}\} & \textcircled{4} &= \{x_{1,1,3}, x_{2,4,2}, x_{3,2,2}, x_{4,5,2}, x_{5,3,2}\} \\ \textcircled{5} &= \{x_{1,2,1}, x_{2,1,2}, x_{3,5,1}, x_{4,3,1}, x_{5,4,2}\} & \textcircled{6} &= \{x_{1,2,1}, x_{2,4,2}, x_{3,5,1}, x_{4,1,2}, x_{5,3,2}\} \\ \textcircled{7} &= \{x_{1,3,1}, x_{2,1,2}, x_{3,2,1}, x_{4,5,2}, x_{5,4,2}\} & \textcircled{8} &= \{x_{1,4,2}, x_{2,1,2}, x_{3,2,2}, x_{4,5,2}, x_{5,3,2}\} \end{aligned}$$

Let \mathbf{z}_1 consist of marked points in all domains except for $D_{12}, D_{13}, D_{30}, D_{49}$. The differentials for the Heegaard diagram $(\Sigma, \boldsymbol{\alpha}, \boldsymbol{\beta}, \mathbf{z}_1)$ along with the domains of the connecting disks are shown in Figure 8 on the left. In this figure, a black arrow from a generator x to a generator y denotes that there is a disk from x to y with a unique holomorphic representative. In fact, the domains associated with all the disks are polygons. The group $H_*(\widehat{CF}(\Sigma, \boldsymbol{\alpha}, \boldsymbol{\beta}, \mathbf{z}_1), \mathfrak{s}_1)$ is thus isomorphic to \mathbb{Z}_2^2 and is generated by $C = \{\textcircled{5}, \textcircled{7}\}$. To compute $\widehat{HF}(M, \mathfrak{s}_1)$, we need to determine the matrices l, n, p , and k in Lemma 3.1. Define the disks $\phi \in \pi_2(\textcircled{3}, \textcircled{7})$ and

$$\phi_1 \in \pi_2(\textcircled{5}, \textcircled{7}), \quad \phi_2 \in \pi_2(\textcircled{5}, \textcircled{6}), \quad \phi_3 \in \pi_2(\textcircled{2}, \textcircled{7}), \quad \phi_4 \in \pi_2(\textcircled{2}, \textcircled{6}), \quad \phi_5 \in \pi_2(\textcircled{5}, \textcircled{1}),$$

of Maslov index 1 by specifying their domains. If $I = \{4, 16, 18, 26, 34, 36, 38, 51, 52\}$ and D is the formal sum $\sum_{i \in I} D_i$, we have

$$\begin{aligned} D(\phi) &= D_0, & D(\phi_1) &= \Sigma - \{D_{12} + D_{14} + D_{30}\}, & D(\phi_2) &= \Sigma - \{D_0 + D_{14}\}, \\ D(\phi_3) &= \Sigma - (D + D_{12} + D_{14} + D_{30}), & D(\phi_4) &= \Sigma - (D + D_0 + D_{14}), & D(\phi_5) &= D + D_{49}. \end{aligned}$$

Then all the disks of index 1 and positive domain between the generators of this complex are the disks ψ_i for $i = 1, 2, 3$, the disk ϕ , the disks ϕ_i for $i = 1, \dots, 5$, the disks $\phi_i - P_1$ for $i = 1, \dots, 4$ and the disks $\phi_i + P_1$ for $i = 1, 2, 5$, see Figure 8 (right). Let

$$\begin{aligned} b_i &= \#\widehat{M}(\phi_i), & \text{for } i = 1, \dots, 5, & & c_i &= \#\widehat{M}(\phi_i - P_1), & \text{for } i = 1, \dots, 4, \\ d_i &= \#\widehat{M}(\phi_i + P_1), & \text{for } i = 1, 2, & \text{and} & c_5 &= \#\widehat{M}(\phi_5 + P_1). \end{aligned}$$

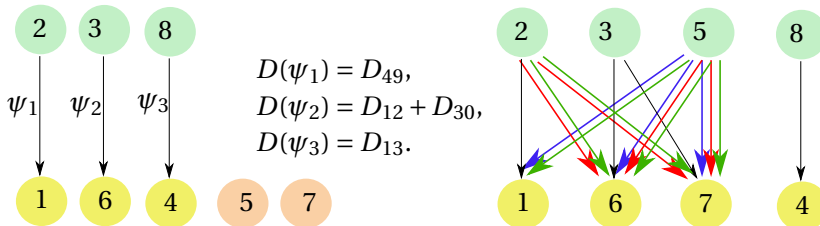


Figure 8. Left: The differential for $(\Sigma, \boldsymbol{\alpha}, \boldsymbol{\beta}, \mathbf{z}_1)$, Right: The differential for $(\Sigma, \boldsymbol{\alpha}, \boldsymbol{\beta}, \mathbf{z})$. The contributions from the disks ϕ_i for $i = 1, \dots, 5$, the disks $\phi_i - P_1$ for $i = 1, \dots, 4$ and the disks $\phi_i + P_1$ for $i = 1, 2, 5$ are denoted with green, red and blue arrows, respectively.

Setting $K = b_4 + c_4 e^{-P_1}$, $N_1 = b_5 + c_5 e^{P_1}$, $N_2 = b_2 + c_2 e^{-P_1} + d_2 e^{P_1}$, $P = b_3 + c_3 e^{-P_1}$ and $L = b_1 + c_1 e^{-P_1} + d_1 e^{P_1}$, it then follows that

$$k = \begin{pmatrix} 0 & 0 & 0 \\ K & 0 & 0 \\ 0 & 0 & 0 \end{pmatrix}, \quad n = \begin{pmatrix} N_1 & 0 \\ N_2 & 0 \\ 0 & 0 \end{pmatrix}, \quad p = \begin{pmatrix} 0 & 0 & 0 \\ P & 1 & 0 \end{pmatrix}, \quad l = \begin{pmatrix} 0 & 0 \\ L & 0 \end{pmatrix}$$

$$\Rightarrow l + p(I + k)^{-1}n = \begin{pmatrix} 0 & 0 \\ L + N_1(P + K) + N_2 & 0 \end{pmatrix}.$$

Note that in this matrix we have

$$\begin{aligned} \star &= L + N_1(P + K) + N_2 = (b_1 + b_2 + b_5 b_3 + b_5 b_4 + c_5 c_3 + c_5 c_4) \\ &\quad + (c_1 + c_2 + b_5 c_3 + b_5 c_4) e^{-P_1} + (d_1 + d_2 + c_5 b_3 + c_5 b_4) e^{P_1}. \end{aligned} \quad (4)$$

The computation of $\widehat{HF}(M, \mathfrak{s}_1)$ is thus reduced to a computation of \star . Consider the disks

$$\begin{aligned} \lambda_1 &\in \pi_2(\textcircled{7}, \textcircled{5}), & \lambda_2 &\in \pi_2(\textcircled{6}, \textcircled{5}), & \lambda_3 &\in \pi_2(\textcircled{7}, \textcircled{2}), \\ \lambda_4 &\in \pi_2(\textcircled{6}, \textcircled{2}), & \lambda_5 &\in \pi_2(\textcircled{1}, \textcircled{5}), & \text{and} & \lambda_6 &\in \pi_2(\textcircled{1}, \textcircled{2}). \end{aligned}$$

which correspond to the domains

$$D(\lambda_i) = \Sigma - D(\phi_i), \quad \text{for } i = 1, \dots, 5 \quad \text{and} \quad D(\lambda_6) = \Sigma - D(\psi_1).$$

The domains of λ_1 and λ_2 are polygons. Then all the positive disks of index 1 in $\pi_2(\textcircled{1}, x)$, $\pi_2(x, \textcircled{5})$, and $\pi_2(x, \textcircled{2})$, with x a generator of $\widehat{CF}(M, \mathfrak{s}_1)$, which the region containing the marked point z are λ_i for $i = 1, \dots, 6$, $\lambda_i + P_1$ for $i = 3, 4, 6$, and $\lambda_i - P_1$ for $i = 5, 6$. Let

$$\begin{aligned} b'_i &= \#\widehat{M}(\lambda_i), & \text{for } i = 3, \dots, 6, & & c'_i &= \#\widehat{M}(\lambda_i + P_1), & \text{for } i = 3, 4, \\ c'_i &= \#\widehat{M}(\lambda_i - P_1), & \text{for } i = 5, 6, & & \text{and} & d'_6 &= \#\widehat{M}(\lambda_6 + P_1). \end{aligned}$$

Consider the Whitney disk classes of index 2

$$\eta_1, \eta'_1, \eta''_1 \in \pi_2(\textcircled{5}, \textcircled{5}), \quad \eta_2, \eta'_2, \eta''_2 \in \pi_2(\textcircled{1}, \textcircled{1}) \quad \text{and} \quad \eta_3, \eta'_3, \eta''_3 \in \pi_2(\textcircled{2}, \textcircled{2})$$

which correspond to the periodic domains

$$D(\eta_i) = \Sigma, \quad D(\eta'_i) = \Sigma - P_1 \quad \text{and} \quad D(\eta''_i) = \Sigma + P_1, \quad \text{for } i = 1, 2, 3.$$

The possible degenerations of η_1, η_1 and η'_1 to positive disks of Maslov index 1 are:

$$\begin{aligned} \eta_1 &= \phi_j * \lambda_j = (\phi_5 + P_1) * (\lambda_5 - P_1), & \text{for } j = 1, 2, 5, \\ \eta'_1 &= (\phi_i - P_1) * \lambda_i = \phi_5 * (\lambda_5 - P_1), & \text{for } i = 1, 2 \quad \text{and} \\ \eta''_1 &= (\phi_i + P_1) * \lambda_i = (\phi_5 + P_1) * \lambda_5, & \text{for } i = 1, 2 \end{aligned}$$

Therefore, the following three equations follow:

$$b_1 + b_2 + b'_5 b_5 + c'_5 c_5 = 0, \quad c_1 + c_2 + c'_5 b_5 = 0 \quad \text{and} \quad d_1 + d_2 + b'_5 c_5 = 0. \quad (5)$$

The possible degenerations of η_2, η'_2 and η''_2 into positive disks of Maslov index 1 are

$$\begin{aligned} \eta_2 &= \lambda_6 * \psi_1 = \lambda_5 * \phi_5 = (\lambda_5 - P_1) * (\phi_5 + P_1) \\ \eta'_2 &= (\lambda_6 - P_1) * \psi_1 = (\lambda_5 - P_1) * \phi_5 \quad \text{and} \\ \eta''_2 &= (\lambda_6 + P_1) * \psi_1 = \lambda_5 * (\phi_5 + P_1). \end{aligned}$$

Therefore, we obtain the following 3 equations

$$b'_6 + b'_5 b_5 + c'_5 c_5 = 0, \quad c'_6 + c'_5 b_5 = 0 \quad \text{and} \quad d'_6 + b'_5 c_5 = 0. \quad (6)$$

Similarly, the possible degeneration of η_3, η'_3 and η''_3 into positive disks of Maslov index 1 are

$$\begin{aligned} \eta_3 &= \phi_i * \lambda_i = (\phi_i - P_1) * (\lambda_i + P_1) = \psi_1 * \lambda_6 \\ \eta'_3 &= (\phi_i - P_1) * \lambda_i = \psi_1 * (\lambda_6 - P_1) \quad \text{and} \\ \eta''_3 &= \phi_i * (\lambda_i + P_1) = \psi_1 * (\lambda_6 + P_1) \quad \text{for } i = 3, 4. \end{aligned}$$

Therefore, we obtain the following 3 equations as well

$$b'_3 b_3 + b'_4 b_4 + c'_3 c_3 + c'_4 c_4 + b'_6 = 0, \quad b'_3 c_3 + b'_4 c_4 + c'_6 = 0 \quad \text{and} \quad c'_3 b_3 + c'_4 b_4 + d'_6 = 0. \quad (7)$$

Let \mathbf{z}'_1 contain a marked point in all the regions of $\Sigma - \boldsymbol{\alpha} - \boldsymbol{\beta}$ except for those appearing in $D(\lambda_3), D(\lambda_4), D(\phi_5)$, and D_{13} and ∂_1 denote the corresponding differential. Note that P_1, P_2 and $P_3 - \Sigma$ may still be considered as a basis for the space of periodic domains. Therefore, the diagram remains admissible for this choice of marked points. Then

$$\partial_1^2 \textcircled{3} = (b'_3 + b'_4) \textcircled{2} \quad \text{and} \quad \partial_1^2 \textcircled{7} = (b_5 + b'_3) \textcircled{1} \quad \Rightarrow \quad b'_3 = b'_4 = b_5. \quad (8)$$

Similarly, let \mathbf{z}'_2 contain a marked point in all the regions of $\Sigma - \boldsymbol{\alpha} - \boldsymbol{\beta}$ except for those appearing in $D(\lambda_3 + P_1), D(\lambda_4 + P_1), D(\phi_5 + P_1)$, and D_{13} and ∂_2 denote the corresponding differential. Then

$$\partial_2^2 \textcircled{3} = (c'_3 + c'_4) \textcircled{2} \quad \text{and} \quad \partial_2^2 \textcircled{7} = (c_5 + c'_3) \textcircled{1} \quad \Rightarrow \quad c'_3 = c'_4 = c_5. \quad (9)$$

It follows from Equations 4-9 that the matrix $l + p(I + k)^{-1}n = 0$. Thus $\widehat{HF}(M, \mathfrak{s}_1) \neq 0$.

6 The second non-trivial Heegaard-Floer group

Let \mathfrak{s}_2 be the Spin^c class which corresponds to $(0, -1, -8)$. The chain complex $\widehat{CF}(M, \mathfrak{s}_2)$ is bigger, in comparison with $\widehat{CF}(M, \mathfrak{s}_1)$, and is generated by the following 72 generators:

$$\begin{array}{lll}
 \textcircled{1} = \{x_{1,1,2}, x_{2,2,4}, x_{3,4,1}, x_{4,5,1}, x_{5,3,2}\} & \textcircled{2} = \{x_{1,1,3}, x_{2,2,5}, x_{3,4,1}, x_{4,5,1}, x_{5,3,2}\} & \textcircled{3} = \{x_{1,1,2}, x_{2,2,5}, x_{3,5,1}, x_{4,3,1}, x_{5,4,1}\} \\
 \textcircled{4} = \{x_{1,1,2}, x_{2,3,2}, x_{3,2,2}, x_{4,5,1}, x_{5,4,1}\} & \textcircled{5} = \{x_{1,1,2}, x_{2,3,2}, x_{3,5,2}, x_{4,2,1}, x_{5,4,1}\} & \textcircled{6} = \{x_{1,1,2}, x_{2,4,1}, x_{3,2,2}, x_{4,5,1}, x_{5,3,1}\} \\
 \textcircled{7} = \{x_{1,1,2}, x_{2,4,1}, x_{3,5,2}, x_{4,2,1}, x_{5,3,1}\} & \textcircled{8} = \{x_{1,1,3}, x_{2,4,1}, x_{3,5,1}, x_{4,2,1}, x_{5,3,2}\} & \textcircled{9} = \{x_{1,2,2}, x_{2,3,2}, x_{3,1,1}, x_{4,5,1}, x_{5,4,2}\} \\
 \textcircled{10} = \{x_{1,2,2}, x_{2,4,2}, x_{3,1,1}, x_{4,5,1}, x_{5,3,1}\} & \textcircled{11} = \{x_{1,3,1}, x_{2,1,1}, x_{3,2,1}, x_{4,4,7}, x_{5,5,1}\} & \textcircled{12} = \{x_{1,3,1}, x_{2,1,1}, x_{3,2,1}, x_{4,4,7}, x_{5,5,2}\} \\
 \textcircled{13} = \{x_{1,3,1}, x_{2,1,1}, x_{3,2,2}, x_{4,4,5}, x_{5,5,1}\} & \textcircled{14} = \{x_{1,3,1}, x_{2,1,1}, x_{3,2,2}, x_{4,4,5}, x_{5,5,2}\} & \textcircled{15} = \{x_{1,3,1}, x_{2,1,1}, x_{3,2,3}, x_{4,4,10}, x_{5,5,1}\} \\
 \textcircled{16} = \{x_{1,3,1}, x_{2,1,1}, x_{3,2,3}, x_{4,4,10}, x_{5,5,2}\} & \textcircled{17} = \{x_{1,3,1}, x_{2,1,1}, x_{3,2,4}, x_{4,4,10}, x_{5,5,1}\} & \textcircled{18} = \{x_{1,3,1}, x_{2,1,1}, x_{3,2,4}, x_{4,4,10}, x_{5,5,2}\} \\
 \textcircled{19} = \{x_{1,3,2}, x_{2,1,1}, x_{3,2,1}, x_{4,4,10}, x_{5,5,1}\} & \textcircled{20} = \{x_{1,3,2}, x_{2,1,1}, x_{3,2,1}, x_{4,4,10}, x_{5,5,2}\} & \textcircled{21} = \{x_{1,3,2}, x_{2,1,1}, x_{3,2,2}, x_{4,4,8}, x_{5,5,1}\} \\
 \textcircled{22} = \{x_{1,3,2}, x_{2,1,1}, x_{3,2,2}, x_{4,4,8}, x_{5,5,2}\} & \textcircled{23} = \{x_{1,3,1}, x_{2,2,3}, x_{3,1,2}, x_{4,5,1}, x_{5,4,2}\} & \textcircled{24} = \{x_{1,3,2}, x_{2,2,3}, x_{3,1,1}, x_{4,5,1}, x_{5,4,2}\} \\
 \textcircled{25} = \{x_{1,3,1}, x_{2,2,1}, x_{3,1,1}, x_{4,4,7}, x_{5,5,1}\} & \textcircled{26} = \{x_{1,3,1}, x_{2,2,1}, x_{3,1,1}, x_{4,4,7}, x_{5,5,2}\} & \textcircled{27} = \{x_{1,3,1}, x_{2,2,1}, x_{3,1,2}, x_{4,4,10}, x_{5,5,1}\} \\
 \textcircled{28} = \{x_{1,3,1}, x_{2,2,1}, x_{3,1,2}, x_{4,4,10}, x_{5,5,2}\} & \textcircled{29} = \{x_{1,3,1}, x_{2,2,2}, x_{3,1,1}, x_{4,4,10}, x_{5,5,1}\} & \textcircled{30} = \{x_{1,3,1}, x_{2,2,2}, x_{3,1,1}, x_{4,4,10}, x_{5,5,2}\} \\
 \textcircled{31} = \{x_{1,3,1}, x_{2,2,3}, x_{3,1,1}, x_{4,4,8}, x_{5,5,1}\} & \textcircled{32} = \{x_{1,3,1}, x_{2,2,3}, x_{3,1,1}, x_{4,4,8}, x_{5,5,2}\} & \textcircled{33} = \{x_{1,3,1}, x_{2,2,4}, x_{3,1,1}, x_{4,4,6}, x_{5,5,1}\} \\
 \textcircled{34} = \{x_{1,3,1}, x_{2,2,4}, x_{3,1,1}, x_{4,4,6}, x_{5,5,2}\} & \textcircled{35} = \{x_{1,3,1}, x_{2,2,4}, x_{3,1,2}, x_{4,4,9}, x_{5,5,1}\} & \textcircled{36} = \{x_{1,3,1}, x_{2,2,4}, x_{3,1,2}, x_{4,4,9}, x_{5,5,2}\} \\
 \textcircled{37} = \{x_{1,3,1}, x_{2,2,5}, x_{3,1,1}, x_{4,4,4}, x_{5,5,1}\} & \textcircled{38} = \{x_{1,3,1}, x_{2,2,5}, x_{3,1,1}, x_{4,4,4}, x_{5,5,2}\} & \textcircled{39} = \{x_{1,3,1}, x_{2,2,5}, x_{3,1,2}, x_{4,4,7}, x_{5,5,1}\} \\
 \textcircled{40} = \{x_{1,3,1}, x_{2,2,5}, x_{3,1,2}, x_{4,4,7}, x_{5,5,2}\} & \textcircled{41} = \{x_{1,3,2}, x_{2,2,1}, x_{3,1,1}, x_{4,4,10}, x_{5,5,1}\} & \textcircled{42} = \{x_{1,3,2}, x_{2,2,1}, x_{3,1,1}, x_{4,4,10}, x_{5,5,2}\} \\
 \textcircled{43} = \{x_{1,3,2}, x_{2,2,4}, x_{3,1,1}, x_{4,4,9}, x_{5,5,1}\} & \textcircled{44} = \{x_{1,3,2}, x_{2,2,4}, x_{3,1,1}, x_{4,4,9}, x_{5,5,2}\} & \textcircled{45} = \{x_{1,3,2}, x_{2,2,5}, x_{3,1,1}, x_{4,4,7}, x_{5,5,1}\} \\
 \textcircled{46} = \{x_{1,3,2}, x_{2,2,5}, x_{3,1,1}, x_{4,4,7}, x_{5,5,2}\} & \textcircled{47} = \{x_{1,3,2}, x_{2,2,5}, x_{3,1,2}, x_{4,4,10}, x_{5,5,1}\} & \textcircled{48} = \{x_{1,3,2}, x_{2,2,5}, x_{3,1,2}, x_{4,4,10}, x_{5,5,2}\} \\
 \textcircled{49} = \{x_{1,3,1}, x_{2,2,3}, x_{3,4,2}, x_{4,1,1}, x_{5,5,1}\} & \textcircled{50} = \{x_{1,3,1}, x_{2,2,3}, x_{3,4,2}, x_{4,1,1}, x_{5,5,2}\} & \textcircled{51} = \{x_{1,3,1}, x_{2,2,3}, x_{3,5,2}, x_{4,1,1}, x_{5,4,2}\} \\
 \textcircled{52} = \{x_{1,3,1}, x_{2,2,5}, x_{3,5,1}, x_{4,1,2}, x_{5,4,1}\} & \textcircled{53} = \{x_{1,3,2}, x_{2,2,4}, x_{3,5,1}, x_{4,1,1}, x_{5,4,2}\} & \textcircled{54} = \{x_{1,4,1}, x_{2,1,2}, x_{3,2,2}, x_{4,5,1}, x_{5,3,1}\} \\
 \textcircled{55} = \{x_{1,4,3}, x_{2,1,1}, x_{3,2,1}, x_{4,5,1}, x_{5,3,2}\} & \textcircled{56} = \{x_{1,4,4}, x_{2,1,1}, x_{3,2,2}, x_{4,5,1}, x_{5,3,2}\} & \textcircled{57} = \{x_{1,4,1}, x_{2,1,2}, x_{3,5,2}, x_{4,2,1}, x_{5,3,1}\} \\
 \textcircled{58} = \{x_{1,4,2}, x_{2,1,1}, x_{3,5,1}, x_{4,2,2}, x_{5,3,2}\} & \textcircled{59} = \{x_{1,4,4}, x_{2,1,1}, x_{3,5,1}, x_{4,2,1}, x_{5,3,1}\} & \textcircled{60} = \{x_{1,4,4}, x_{2,1,1}, x_{3,5,2}, x_{4,2,1}, x_{5,3,2}\} \\
 \textcircled{61} = \{x_{1,4,2}, x_{2,2,3}, x_{3,1,1}, x_{4,5,1}, x_{5,3,1}\} & \textcircled{62} = \{x_{1,4,2}, x_{2,2,4}, x_{3,1,2}, x_{4,5,1}, x_{5,3,2}\} & \textcircled{63} = \{x_{1,4,3}, x_{2,2,1}, x_{3,1,1}, x_{4,5,1}, x_{5,3,2}\} \\
 \textcircled{64} = \{x_{1,4,3}, x_{2,2,4}, x_{3,1,1}, x_{4,5,1}, x_{5,3,1}\} & \textcircled{65} = \{x_{1,4,3}, x_{2,2,5}, x_{3,1,2}, x_{4,5,1}, x_{5,3,2}\} & \textcircled{66} = \{x_{1,4,4}, x_{2,2,5}, x_{3,1,1}, x_{4,5,1}, x_{5,3,1}\} \\
 \textcircled{67} = \{x_{1,4,1}, x_{2,2,5}, x_{3,5,1}, x_{4,1,2}, x_{5,3,2}\} & \textcircled{68} = \{x_{1,4,2}, x_{2,2,1}, x_{3,5,1}, x_{4,1,1}, x_{5,3,2}\} & \textcircled{69} = \{x_{1,4,2}, x_{2,2,4}, x_{3,5,1}, x_{4,1,1}, x_{5,3,1}\} \\
 \textcircled{70} = \{x_{1,4,2}, x_{2,2,4}, x_{3,5,2}, x_{4,1,1}, x_{5,3,2}\} & \textcircled{71} = \{x_{1,4,3}, x_{2,2,5}, x_{3,5,1}, x_{4,1,1}, x_{5,3,1}\} & \textcircled{72} = \{x_{1,4,3}, x_{2,2,5}, x_{3,5,2}, x_{4,1,1}, x_{5,3,2}\}
 \end{array}$$

Let \mathbf{z}_1 consist of a marked point in all regions of the Heegaard diagram except for D_i with $i = 4, 16, 17, 21, 22, 23, 25, 26, 27, 36, 37, 38, 58, 59, 60, 61, 62, 63, 64, 68$. A neighborhood of these

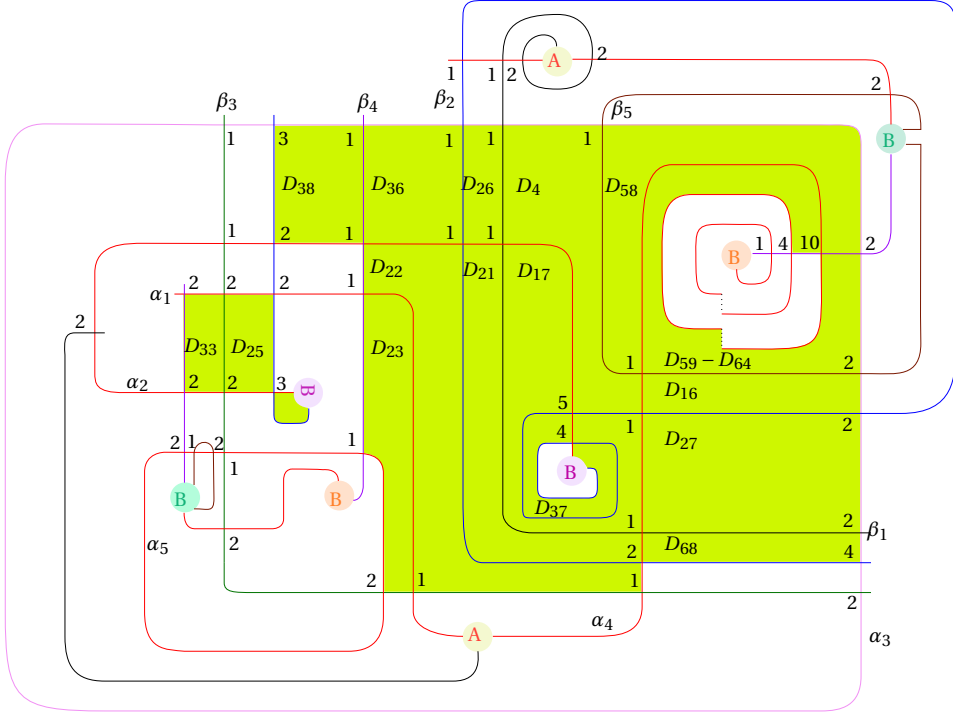


Figure 9. Part of the Heegaard diagram, where the marked points \mathbf{z}_1 are in the domains other than those in green.

latter domains is illustrated in Figure 9, where the aforementioned domains are colored green.

The differential corresponding to the Heegaard diagram $(\Sigma, \alpha, \beta, \mathbf{z}_1)$ is illustrated in Figure 10. In fact, most of the positive Whitney disks of Maslov index 1 for $(\Sigma, \alpha, \beta, \mathbf{z}_1)$, which connect two of the aforementioned 72 generators have polygonal domains, and their contribution to the differential is thus equal to 1. There are precisely 12 disks ϕ_i for $i = 1, \dots, 7$, and ϕ'_j for $j = 1, 2, 5, 6, 7$, with non-polygonal domains, where we have

$$\begin{aligned}
 \phi_1 &\in \pi_2((21), (45)), & \phi'_1 &\in \pi_2((22), (46)), & \phi_2 &\in \pi_2((13), (37)), & \phi'_2 &\in \pi_2((14), (38)), \\
 \phi_3 &\in \pi_2((3), (1)), & \phi_4 &\in \pi_2((71), (64)), & \phi_5 &\in \pi_2((47), (43)), & \phi'_5 &\in \pi_2((48), (44)), \\
 \phi_6 &\in \pi_2((39), (33)), & \phi'_6 &\in \pi_2((40), (34)), & \phi_7 &\in \pi_2((35), (31)), & \phi'_7 &\in \pi_2((36), (32)).
 \end{aligned}$$

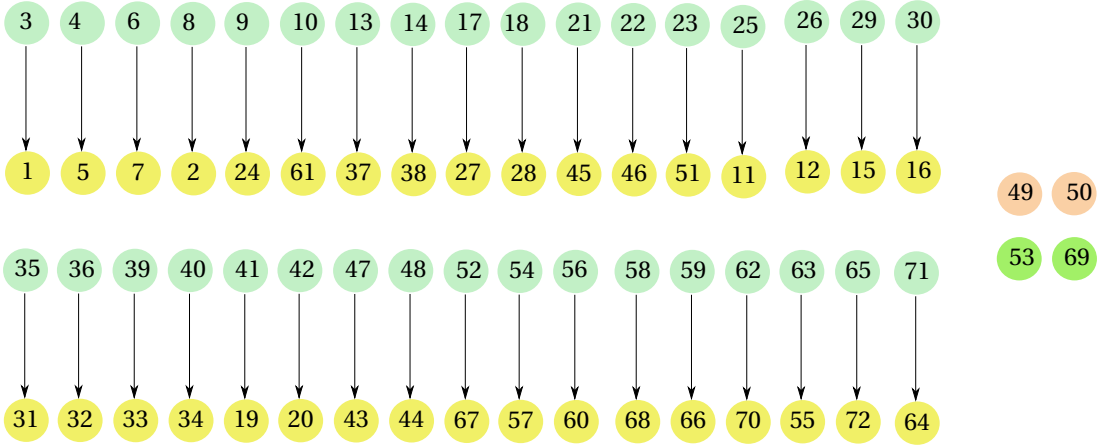


Figure 10. The differential corresponding to the diagram $(\Sigma, \alpha, \beta, \mathbf{z}_1)$.

The domains associated with these disks are

$$\begin{aligned}
 D(\phi_1) &= D(\phi'_1) = D_4 + D_{16} + D_{58} + D_{59} + D_{60} + D_{61}, & D(\phi_2) &= D(\phi'_2) = D(\phi_1) + D_{62} + D_{63} + D_{64}, \\
 D(\phi_3) &= D_4 + D_{17} + D_{21} + D_{22} + D_{23} + D_{26} + D_{36}, & D(\phi_4) &= D_4 + D_{17}, \\
 D(\phi_5) &= D(\phi'_5) = D_4 + D_{16} + D_{17} + D_{27} + D_{58} + D_{59}, & D(\phi_6) &= D(\phi'_6) = D(\phi_5) + D_{60} + D_{61} + D_{62}, \\
 D(\phi_7) &= D(\phi'_7) = D(\phi_5) + D_{60}.
 \end{aligned}$$

By Lemma 4.1, $\#\widehat{M}(\phi_i) = \#\widehat{M}(\phi'_j) = 1$, for $i = 1, \dots, 4$ and $j = 1, 2$. Moreover, by Lemma 4.2, $\#\widehat{M}(\phi_i) = \#\widehat{M}(\phi'_i) = 1$ for $i = 5, 6, 7$. Thus, the differential is as illustrated in Figure 10 and $H_*(\widehat{CF}(\Sigma, \alpha, \beta, \mathbf{z}_1))$ is generated by

$$C = \{C_1 = \textcircled{49}, C_2 = \textcircled{50}, C_3 = \textcircled{53}, C_4 = \textcircled{69}\}.$$

To compute $\widehat{HF}(M, s_2)$, we need to determine the matrices l , n , p , and k in the Lemma 3.1. All possible positive disks with Maslov index 1 between the generators in C are

$$\begin{aligned}
 \psi'_1, \psi_1 &\in \pi_2(\textcircled{49}, \textcircled{50}), & \psi'_2, \psi_2 &\in \pi_2(\textcircled{53}, \textcircled{69}), \\
 \psi_3 &\in \pi_2(\textcircled{49}, \textcircled{53}), & \psi_4 &\in \pi_2(\textcircled{50}, \textcircled{69}).
 \end{aligned}$$

For $i = 1, 2$, the domain associated with ψ'_i is a polygon. The domain associated with ψ_1 is shown in Figure 11 as the union of yellow, blue and pink regions. By Lemma 4.3, $\#\widehat{M}(\psi_1) = 1$. The domain associated with ψ_3 is shown in Figure 11 as the union of blue, brown and pink

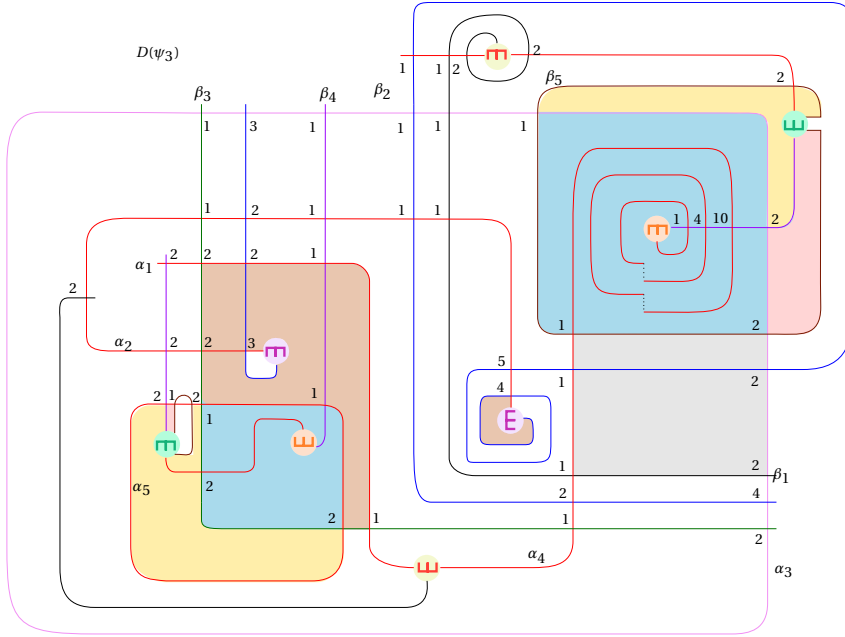


Figure 11. If I_1, I_2, I_3, I_4 and I_5 denote the set of indices of domains colored yellow, blue, pink, grey, and brown respectively, the domains associated with ψ_1, ψ_3 and ψ_6 are given by $D(\psi_1) = \sum_{i \in I_1 \cup I_2 \cup I_3} D_i$, $D(\psi_3) = \sum_{i \in I_2 \cup I_3 \cup I_5} D_i$ and $D(\psi_6) = \sum_{i \in I_2 \cup I_4 \cup I_5} D_i$.

regions. Setting $V = \#\widehat{M}(\psi_3)$, we find

$$l = \begin{pmatrix} 0 & 0 & 0 & 0 \\ 1 + e^{P_1} & 0 & 0 & 0 \\ V & 0 & 0 & 0 \\ 0 & * & * & 0 \end{pmatrix}.$$

Let A and B denote the chain complexes generated by all the generators colored in light green and yellow in Figure 10, respectively. Denote the generators of A and B by A_i and B_i , respectively. We may choose the labeling of the aforementioned generators of A and B such that k is a lower triangular matrix. Therefore,

$$p(I + k)^{-1}n = pn + pkn + pk^2n + \dots$$

For $j \geq 0$, since the coefficients are in \mathbb{Z}_2 , each non-zero entry in $pk^j n$ is of the form

$$(pk^j n)_{wv} = \sum_{r_1, \dots, r_{j+1}} p_{wr_1} k_{r_1 r_2} \dots k_{r_j r_{j+1}} n_{r_{j+1} v},$$

and implies the existence of positive disks λ_t of Maslov index 1 for $t = 1, \dots, j + 1$, where

$$\lambda_1 \in \pi_2(C_v, B_{r_{j+1}}), \quad \lambda_{j+2} \in \pi_2(A_{r_1}, C_w) \quad \text{and} \quad \lambda_t \in \pi_2(A_{r_t}, B_{r_{t-1}}), \quad t = 2, \dots, j + 1.$$

and $\#\widehat{M}(\lambda_t) = 1$. In particular, $D(\lambda_t) > 0$ for all t and

$$D(\lambda_t) \subset \sum_{t=1}^{j+2} D(\lambda_t) = \sum_{t=1}^{j+1} D(\lambda'_t) + D(\lambda) \pm D(P_1), \quad \mu(\lambda_t) = 1, \quad D(\lambda_t) > 0, \quad (10)$$

for some positive Whitney disks $\lambda'_t \in \pi_2(A_{r_t}, B_{r_t})$ and $\lambda \in \pi_2(C_v, C_w)$ of Maslov index 1. Potentially, there are only two such sequences satisfy (10), which are shown in Figure 12. Here $\psi_5 \in \pi_2((49), (51))$ is a disk with a polygonal domain. The domain associated with the disk $\psi_6 \in \pi_2((23), (53))$ is shown in Figure 11 as the union of grey, brown and blue regions.

Lemma 6.1. *With the above notation in place, we have $\#\widehat{M}(\psi_3) = \#\widehat{M}(\psi_6)$.*

Proof. The domains associated with ψ_3 and ψ_6 are extended in two ways in Figure 13. The domains D_i^\bullet for $\bullet = a, b, c$ and d denote the components of the regions colored pink, grey, yellow and green, respectively. They determine the domains of Whitney disks η_a, η_b, η_c and η_d , respectively, with domains $D(\eta_\bullet) = \sum_i D_i^\bullet$. Note that for $\bullet = a, c$ the values of i are in $\{1, \dots, 8\}$, while for $\bullet = b, d$ the values of i are in $\{1, \dots, 4\}$. The possible degenerations for the disks η_a, η_b, η_c and η_d are given by

$$\eta_\bullet = \phi_1^\bullet * \sigma_1^\bullet = \sigma_2^\bullet * \phi_2^\bullet = \sigma_3^\bullet * \phi_3^\bullet \quad \bullet = a, c,$$

$$\eta_\bullet = \phi_1^\bullet * \sigma_1^\bullet = \sigma_2^\bullet * \phi_2^\bullet = \phi_3^\bullet * \sigma_3^\bullet \quad \bullet = b, d,$$

where the corresponding domains are given by

$$\begin{aligned} D(\phi_1^\bullet) &= \sum_{j=1}^5 D_j^\bullet, & D(\phi_2^\bullet) &= D_1^\bullet + \sum_{j=3}^8 D_j^\bullet, & D(\phi_3^\bullet) &= D_1^\bullet + D_2^\bullet + D_3^\bullet + D_6^\bullet \\ D(\sigma_3^\bullet) &= D_4^\bullet + D_5^\bullet + D_7^\bullet + D_8^\bullet, & D(\phi_1^\star) &= D_1^\star + D_2^\star + D_3^\star, & D(\phi_2^\star) &= D_1^\star + D_3^\star + D_4^\star, \\ \text{and} & & D(\phi_3^\star) &= D_1^\star + D_2^\star + D_4^\star \end{aligned}$$

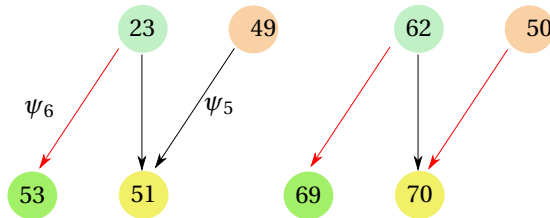


Figure 12. Potential sequences of disks corresponding to non-zero summands $p_{wr_1} k_{r_1 r_2} \dots k_{r_j r_{j+1}} n_{r_{j+1} v}$ in $(pk^j n)_{wv}$.

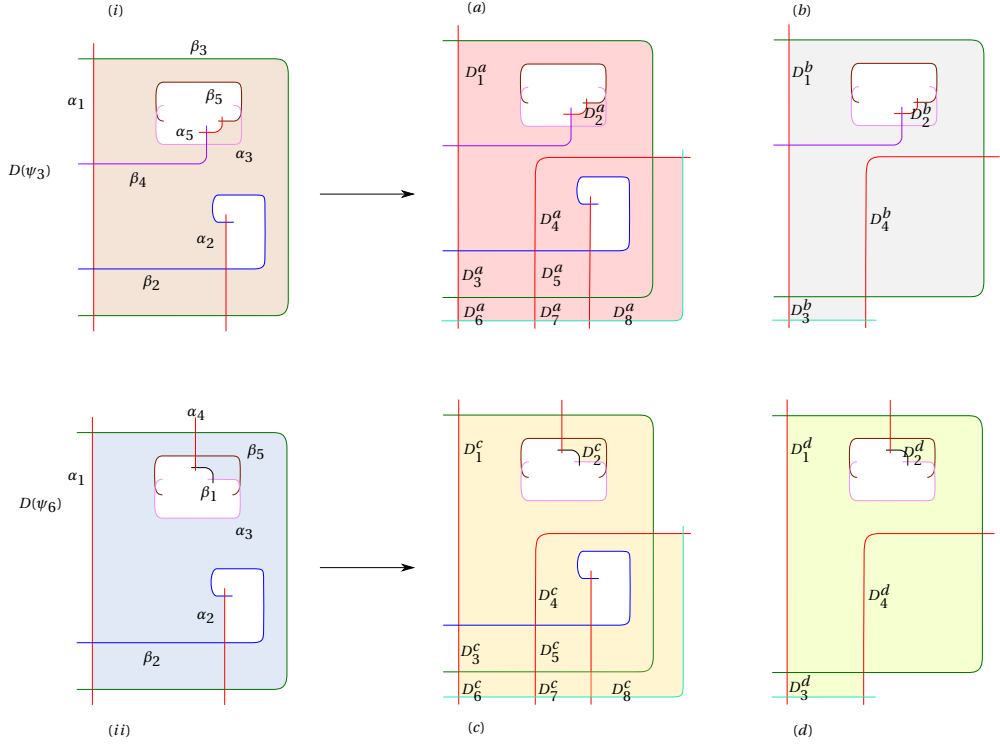


Figure 13. Domains associated with disks $\eta_a, \eta_b, \eta_c, \eta_d$, in (a), (b), (c), (d), respectively.

for $\bullet = a, c$ and $\star = b, d$, while the domains associated with $\sigma_j^a, \sigma_j^c, \sigma_i^b$ and σ_i^d are polygons for $j = 1, 2$ and $i = 1, 2, 3$. By Lemma 4.1, we also have $\#\widehat{M}(\sigma_3^\bullet) = 1$, $\bullet = a, c$. Therefore

$$\sum_{i=1}^3 \#\widehat{M}(\phi_i^\bullet) = 0 \quad \text{for } \bullet = a, b, c, d. \quad (11)$$

On the other hand, we have

$$\begin{aligned} D(\phi_1^a) &= D(\psi_3), & D(\phi_1^c) &= D(\psi_6), & D(\phi_2^a) &= D(\phi_2^c), & D(\phi_2^b) &= D(\phi_2^d), \\ D(\phi_3^a) &= D(\phi_1^b), & D(\phi_3^c) &= D(\phi_1^d), & \text{and} & & D(\phi_3^b) &= D(\phi_3^d). \end{aligned}$$

Thus by 11, we have $V = \#\widehat{M}(\psi_3) = \#\widehat{M}(\psi_6)$. □

Having established Lemma 6.1, we conclude that

$$p(I+k)^{-1}n = \begin{pmatrix} 0 & 0 & 0 & 0 \\ 0 & * & * & * \\ V & * & * & * \\ 0 & * & * & * \end{pmatrix} \Rightarrow l + p(I+k)^{-1}n = \begin{pmatrix} 0 & 0 & 0 & 0 \\ 1 + e^{P_1} & * & * & * \\ 0 & * & * & * \\ 0 & * & * & * \end{pmatrix}.$$

This means that $\textcircled{49}$ survives in $\widehat{HF}(M, \mathfrak{s}_2)$, and the latter group is thus non-trivial.

References

- [AC65] J. J. Andrews and M. L. Curtis. Free groups and handlebodies. *Proc. Amer. Math. Soc.*, 16:192–195, 1965.
- [AE15] Akram S. Alishahi and Eaman Eftekhary. A refinement of sutured Floer homology. *J. Symplectic Geom.*, 13(3):609–743, 2015.
- [Bag] Neda Bagherifard. Three-manifolds with boundary and the Andrews-Curtis transformations. *preprint, available at arXiv:2109.13844v1*.
- [BM93] R. G. Burns and Olga Macedońska. Balanced presentations of the trivial group. *Bull. London Math. Soc.*, 25(6):513–526, 1993.
- [Bro84] Ronald Brown. Coproducts of crossed p -modules: Applications to second homotopy groups and to the homology of groups. *Topology*, 23(3):337–345, 1984.
- [Eft15] Eaman Eftekhary. Floer homology and splicing knot complements. *Algebr. Geom. Topol.*, 15(6):3155–3213, 2015.
- [Eft18] Eaman Eftekhary. Bordered Floer homology and existence of incompressible tori in homology spheres. *Compos. Math.*, 154:1222–1268, 2018.
- [HAM93] Cynthia Hog-Angeloni and Wolfgang Metzler. The Andrews-Curtis conjecture and its generalizations, volume 197 of *London Math. Soc. Lecture Note Ser.* Cambridge Univ. Press, Cambridge, 1993.
- [HRW16] Jonathan Hanselman, Jacob Rasmussen, and Liam Watson. Bordered Floer homology for manifolds with torus boundary via immersed curves. *preprint, available at arXiv:1604.03466v2*, 2016.
- [Juh06] Andras Juhász. Holomorphic discs and sutured manifolds. *Algebr. Geom. Topol.*, 6:1429–1457, 2006.
- [Lek13] Yanki Lekili. Heegaard Floer homology of broken fibrations over the circle. *Advances in Mathematics*, 244:268–302, 2013.
- [MMS02] Alexei D. Myasnikov, Alexei G. Myasnikov, and Vladimir Shpilrain. On the Andrews-Curtis equivalence. *Combinatorial and geometric group theory (New York, 2000/Hoboken, NJ, 2001)*, volume 296 of *Contemp. Math.*, pages 183–198. Amer. Math. Soc., Providence, RI, 2002.
- [MS99] Charles F. Miller, III and Paul E. Schupp. Some presentations of the trivial group. *Groups, languages and geometry (South Hadley, MA, 1998)*, volume 250 of *Contemp. Math.*, pages 113–115. Amer. Math. Soc., Providence, RI, 1999.
- [OS04a] P. Ozsváth and Z. Szabó. Holomorphic disks and genus bounds. *Geometry and Topology*, 8:311–334, 2004.

- [OS04b] Peter Ozsváth and Zoltán Szabó. Holomorphic disks and topological invariants for closed three-manifolds. *Ann. of Math. (2)*, 159(3):1027–1158, 2004.
- [SW10] Sucharit Sarkar and Jiajun Wang. An algorithm for computing some Heegaard Floer homologies. *Ann. of Math. (2)*, 171(2):1213–1236, 2010.
- [Thu86] William P Thurston. A norm for the homology of 3-manifolds. *Mem. Amer. Math. Soc.*, 59(339):i–vi and 99–130, 1986.
- [Wri75] Perrin Wright. Group presentations and formal deformations. *Trans. Amer. Math. Soc.*, 208:161–169, 1975.

Neda Bagherifard

email: neda.bagherifard@gmail.com

Eaman Eftekhary

School of Mathematics, Institute for Research in Fundamental Sciences (IPM), P. O. Box 19395-5746, Tehran, Iran

email: eaman@ipm.ir